LABORATORY AND NUMERICAL MODELING USED TO CHARACTERIZE LEAKAGE IN UNDERGROUND COAL MINES

by

Miles Stephens

A thesis submitted to the faculty of
The University of Utah
in partial fulfillment of the requirements for the degree of

Master of Science

Department of Mining Engineering

The University of Utah

May 2011

The University of Utah Graduate School

STATEMENT OF THESIS APPROVAL

The thesis of **Miles Stephens**

has been approved by the following supervisory committee members:

Felipe Calizaya	, Chair	**05/14/2010** Date Approved
Michael G. Nelson	, Member	**05/14/2010** Date Approved
Erich U. Peterson	, Member	**05/14/2010** Date Approved

and by **Michael G. Nelson** , Chair of the Department of **Mining Engineering**

and by Charles A. Wight, Dean of The Graduate School.

ABSTRACT

Stoppings and other control devices used in underground mines can be viewed as air paths with high resistance. The amount of air that leaks through these devices depends on various factors including the type of construction materials used, workmanship, and stopping inspection and maintenance. Improperly constructed and poorly maintained structures will significantly lower this resistance and cause undue leakage.

The circumstances of a real-world mine rarely exhibit the ideal conditions needed to obtain the most accurate measurements. The airflows and pressure drops in an underground mine are subject to considerable variation due to movement of equipment, opening of vent doors, and other changes. In addition, mine layouts are often extremely complex and may be such that the airflow profile at the location where a measurement is required is not fully developed. This can make it so that fluid-flow laws are not truly applicable. Nevertheless, a practical effort must be made.

In ventilation planning, resistance values are often measured in the field or in an experimental lab. These measurements were used in a simulated model which was calibrated to match the field conditions. This calibrated model was then used to further evaluate the pressure/quantity requirements for future mining scenarios.

Experimental tests conducted at the University of Utah’s coal mine model indicate that for a set of similar stoppings, the trend of pressure drop across the stoppings decreases with distance from the main fan. The trend resembles an exponential decay

curve more than a linear one. The resistance values measured in the lab are directly correlated to real world measurements by a physical scale factor of 1:625.

A CFD model was calibrated to within 5% of the lab measurements. Additional analyses with the CFD model also indicated that with increasing distance from the fan, both pressure drop and leakage flow through the stoppings exhibit an exponential decay function. A single main fan system was compared with a system having a main fan plus a booster fan. The results indicate that the booster fan creates a substantial reduction in pressure drop across the stoppings and a reduction in leakage as well.

A VNETPC model of a two-entry development section was used to further characterize leakage flow in terms of progressive mine development, building materials used, and engineering design strategies. From these analyses, a recommended method of prioritizing life of mine engineering designs and leakage reduction methods to be focused in the critical leakage areas was developed. These critical leakage areas are identified as a proportional distance from the main fan. This method is applicable to existing large or extensive mines as well as future projects.

Dedicated to my parents Wendell and Beth, my dear wife Victoria for her patience, love and support, and to my children.

TABLE OF CONTENTS

LIST OF TABLES

LIST OF FIGURES

ACKNOWLEDGEMENTS

I would first like to express my sincere appreciation to my father for his guidance and advice, and for being the one who originally suggested that I further my academics. Were it not for his influence, I would never have started down this path.

I would next like to express my abundant thankfulness for my committee chair, Dr. Felipe Calizaya. He contributed with his knowledge, skill, expertise, time, patience, and much needed encouragement. I owe him a debt of gratitude for providing help and guidance on this project, and many others. He has been a valuable mentor, not just for my academic career, but for many other aspects of my personal life as well.

I would like to further extend my appreciation to my other committee members: Dr. Mike Nelson and Dr. Erich Peterson, as well as to Dr. Kim McCarter and Dr. Bill Pariseau. Each has contributed significantly to my academic achievements.

Acknowledgement for financial support is given to the William C. Browning Graduate Scholarship, the National Institute for Occupational Safety and Health (NIOSH), and the Western Small Mines Safety Program.

Special recognition is given to Mr. Robert Byrns for his time spent in constructing the laboratory model, and to my good friend Arkadius Sutra Tarigan for his assistance on the field surveys conducted, but more importantly for his companionship. I also appreciate the friendship of all of the other graduate students as well as Pamela Hoffman.

Finally, and above all, I would like to express my love and appreciation to my dear wife Victoria for her constant encouragement, patience, love and sacrifice; and for our children: Caleb and Teddy.

1 INTRODUCTION

Every underground mine contains harmful contaminants, such as toxic or flammable gases, dust, fumes, smoke, heat or radiation. The fundamental purpose of the underground ventilation system is to provide the quantity and quality of air required to dilute the contaminants to safe concentrations where personnel are required to work or travel. In the United States, mines are governed by Title 30 of the Code of Federal Regulations (30 CFR), under which each mine must have an approved mine ventilation plan. Among other things, the mining plan must specify the minimum quantities of fresh air that must be delivered to each working section. But the quantity of air required at the workings is only a portion of the total quantity that must be induced by the fan. Any quantity of air that passes through the main fan but is not usefully employed somewhere in the mine is considered leakage. And while leakage cannot be completely eliminated, it can be significantly reduced with good ventilation practices, proper installation of ventilation control structures, and appropriate planning.

This study presents the results of pressure-quantity (P-Q) surveys conducted in two underground coal mines (Mines A and B), the flow characteristics observed in a lab model simulating a coal mine, and various leakage flow patterns generated using a computational fluid dynamics (CFD) based numerical simulator. The results of the measurements are analyzed, the flow characteristics evaluated, and the factors affecting the leakage quantity identified.

1.1 *Statement of Problems*

Air leakage in underground mines commonly varies between 25–90% (McPherson, 1993). The cost associated with operating a mine fan is dependent on the total quantity of air passing through it as well as the pressure differential induced. As mine development progresses, supplying additional quantities of air will require increasing the fan pressure, thus increasing the leakage quantity and the power requirement. A 10% increase in airflow rate requires a 21% increase in fan pressure and 33% increase in power requirement. Seeber (2002) demonstrates that 10%, 20%, and 30% reductions in leakage volume results in 133%, 171%, and 217% reduction in operating costs, respectfully. Schophaus et al. (2005) estimated that the life-of-mine cost difference between "poor" and "good" stoppings may be on the order of $50 to 100 million (base 2004).

There are three aspects of the problem of leakage that are discussed: leakage paths, leakage in coal mines, and the areas in a mine where the majority of leakage occurs.

1.1.1 Leakage Paths

Airflow currents follow the path of least resistance. Directing air to where it is needed is accomplished by installing highly resistant structures (control devices) that prevent it from flowing to where it is not needed. These control devices include both permanent and temporary structures such as stoppings, regulators, overcasts, seals, and face curtains. Each of these structures as well as others will be discussed in more detail in Chapter 2.

A leakage path is defined as any material or ventilation control device through which air leakage occurs. Assuming a pressure difference is applied across a completed structure, four potential flow paths can be visualized (Martinson, 1985):

1. diffusion paths through porous wall material;
2. cracks in building blocks, between blocks, and between peripheral wall surfaces and surrounding coal or rock surfaces;
3. diffusion paths through porous coal or rock; and
4. fractures within the surrounding coal and rock.

This demonstrates that inevitably, some amount of airflow cannot be blocked, resulting in air that is short-circuited through and around the control devices and lost in the form of leakage. Also, it shows that the characteristics of each device impact a mine's overall leakage. The quantity of air that leaks through a device depends on its resistance to airflow as well as the amount of pressure that is applied.

The resistance of a leakage path is dependent on the mechanical and physical properties of the building materials and the building techniques and quality of workmanship used. An extensive amount of research was conducted by the US Bureau of Mines (USBM) for the purpose of determining which materials are most suitable for use as stoppings, proper construction techniques, and leakage investigations (Kawenski et al., 1963, 1965, 1966; Timko, 1983). At that time, concrete and wood were the most widely used, with wet-stacked concrete being recommended. Since that time, a number of other materials have gained popularity including steel, foam, and a variety of light-weight cementitious materials: Steel Kennedy panels (Kennedy, 1996), Omega-384 blocks (Tien, 1996), and hollow cinder blocks are the types most commonly used in coal mines today.

The quality of workmanship exercised during stopping installation and the ensuing maintenance are key factors of resistance. Regardless of mechanical and physical properties, if controls are not installed properly, their structural integrity deteriorates rapidly over time, requiring excessive and endless repair costs. As stated earlier, air will travel the path of least resistance. So carelessly leaving cracks around a stopping's perimeter, a doorway, or between blocks allows undue leakage to occur.

1.1.2 Leakage in Coal Mines

Underground coal mines are developed using the room and pillar method where intake, belt, and return entries are developed in parallel. These entries are separated by stoppings constructed in connecting crosscuts. Coal miners are faced with a multifaceted problem in terms of ventilation requirements. Within the active development section, fresh air is directed to each cutting face using brattice cloth face curtains or ventilation tubing. As a single entry is developed, prior to making a connecting crosscut, it becomes increasingly difficult to supply the amount of air required because the entry is a dead end. From experience, miners working in the development section often have a tendency to want to develop pillars no more than about 36.6 m (120 ft) in length because it is easier to ventilate the faces during the development cycle. However, by developing shorter pillars rather than longer ones, the mine will in the long-term have a greater number of leakage paths. In coal mines, air leakage averages over 50% (Richardson et al., 1997) whereas in metal mines, leakage is typically 30% or less (Calizaya et al., 2001, Van der Bank, 1983). This inefficient utilization of air in coal mines is largely attributed to the vast number of ventilation control devices required.

In addition to the number of stoppings needed, difficulty in supplying adequate amounts of air to the working sections is also due to constraints on extraction widths and heights. Coal mine entries are limited to an extraction width of 6.1 m (20 ft) (30 CFR § 75.206(a)(1)). The extraction height is usually limited by the seam thickness, which is on average, not more than 3.7 m (12 ft) in the western U.S. and about 1.5 m (5 ft) in the eastern U.S. This limited extraction height makes it difficult to use auxiliary ventilation systems in these mines. Therefore, supplying additional quantities of air may require developing additional parallel entries, which is costly.

1.1.3 Leakage Location

Although each individual stopping is a flow path that allows leakage, air leaks through some significantly more than others. This leakage quantity is dependent upon the pressure difference across it and its ability to resist flow. High pressure differentials in a mine are located near fan installations, surface openings (particularly shafts), air crossings, and through old workings. The pressure profile of a mine will indicate the high-pressure areas and thus areas where leakage will most likely occur. However, these profiles change gradually as mining progresses, making it difficult to identify a distinct location where leakage is no longer relatively insignificant. Nevertheless, Kawenski et al. (1963), Kharkar et al. (1974), Coetzer (1985), and Tien (1996) make the following key points concerning leakage:

1. It is not uncommon for underground coal mines to have 50-60% overall leakage.
2. Leakage losses are significantly higher in the vicinity of the fan.
    - Generally 75% of the total leakage occurs in the first half of the mine workings (halfway between the fan and the active workings).

- As much as 80% of the mine air leakage may happen in the vicinity and within a 610 m (2,000 ft.) radius of the fan shaft.

3. The pressure differential across a stopping has the greatest influence on leakage through it.
4. Air leakage is significantly reduced by coating a stopping with sealant.
5. Leakages are not the same in every mine.

1.2 *Thesis Objective*

Although leakage can be a problem in any underground mine, this thesis focuses on the high levels of leakage that occur in coal mines. The main objective is to demonstrate that leakage can be significantly reduced by improving three main areas: (1) improving building methods and materials used for ventilation control devices, (2) improving mine design, particularly in the high-pressure areas near the fan, and (3) optimizing the positions and duties of main fans and utilizing booster fans. This is accomplished by characterizing leakage flows based on field surveys, a laboratory model, and numerical modeling. This flow characterization is used to develop guidelines that ventilation engineers can use to aid them in ventilation planning.

2 COAL MINE VENTILATION SYSTEMS

Every new mining project experiences a high-cost development or investment phase before reaching the lucrative low-cost, production phase. In the case of underground mine projects, efforts to minimize these initial costs often lead to insufficient ventilation planning. As a result, leakage becomes a very high operating cost throughout the mine's life. This cost is often overlooked however, because leakage is an inherent part of underground ventilation. But with proper planning, strategic initial mine development, and installation and maintenance of airflow controls, this high operating cost can be minimized. For this purpose, a basic understanding of mine ventilation systems is necessary.

For a volume of air to move from one location in a mine to another, there must be a difference in pressure between the two points. The air moves from the high-pressure point to the low-pressure point. In mountainous terrain, if there is a large enough difference between the pressure underground and the atmospheric pressure, significant amounts of air may enter an opening at one elevation and exit at another. This is called natural ventilation. Airflow from natural ventilation may become inert or even reverse direction from summer to winter or even from day to night. Mining usually requires a more constant and reliable airflow pattern than natural ventilation can provide, so a pressure differential is induced mechanically using large main fans.

A number of essential elements are required of a ventilation system in any underground mine. These elements include fans, intake air paths, return air paths,

working faces, and ventilation controls. These elements are shown on the mine map depicted in Figure 2.1. This mine has three active mining sections: two development sections and one longwall section. Figure 2.1 also shows a caved area (gob) that has been isolated from the rest of the mine using seals. Finally, in this example, the mine utilizes a single exhausting main fan.

2.1 *Mine Airways*

A coal mine ventilation system generally consists of three airway types: intake, return, and neutral (belt). On the mine map depicted in Figure 2.1, the intake airways are shown in blue, the return airways in red, and the belt entries in green. The U.S. mining laws require that each of these airways remain separate and distinct. This is done through the use of stoppings, some of which contain doors as indicated in Figure 2.1.

Fresh air enters the mine through one or more connections to the surface. In the example in Figure 2.1, there is only one surface portal. The air enters the intake airways at the surface portal and flows to the working areas (anywhere pollutants enter the system). Ventilation structures are used to direct the air, forcing it to move in the desired directions and at desired velocities to safely ventilate all mine sections. An example of a 5-entry development section is illustrated in Figure 2.2. The two left entries are used for return air, the middle entry contains the conveyor belt and is used for neutral air, and the two right entries are used for intake air. Each of the three airways is separated by a row of permanent stoppings with the exception of the last two crosscuts which are ventilated using temporary structures for active mining access.

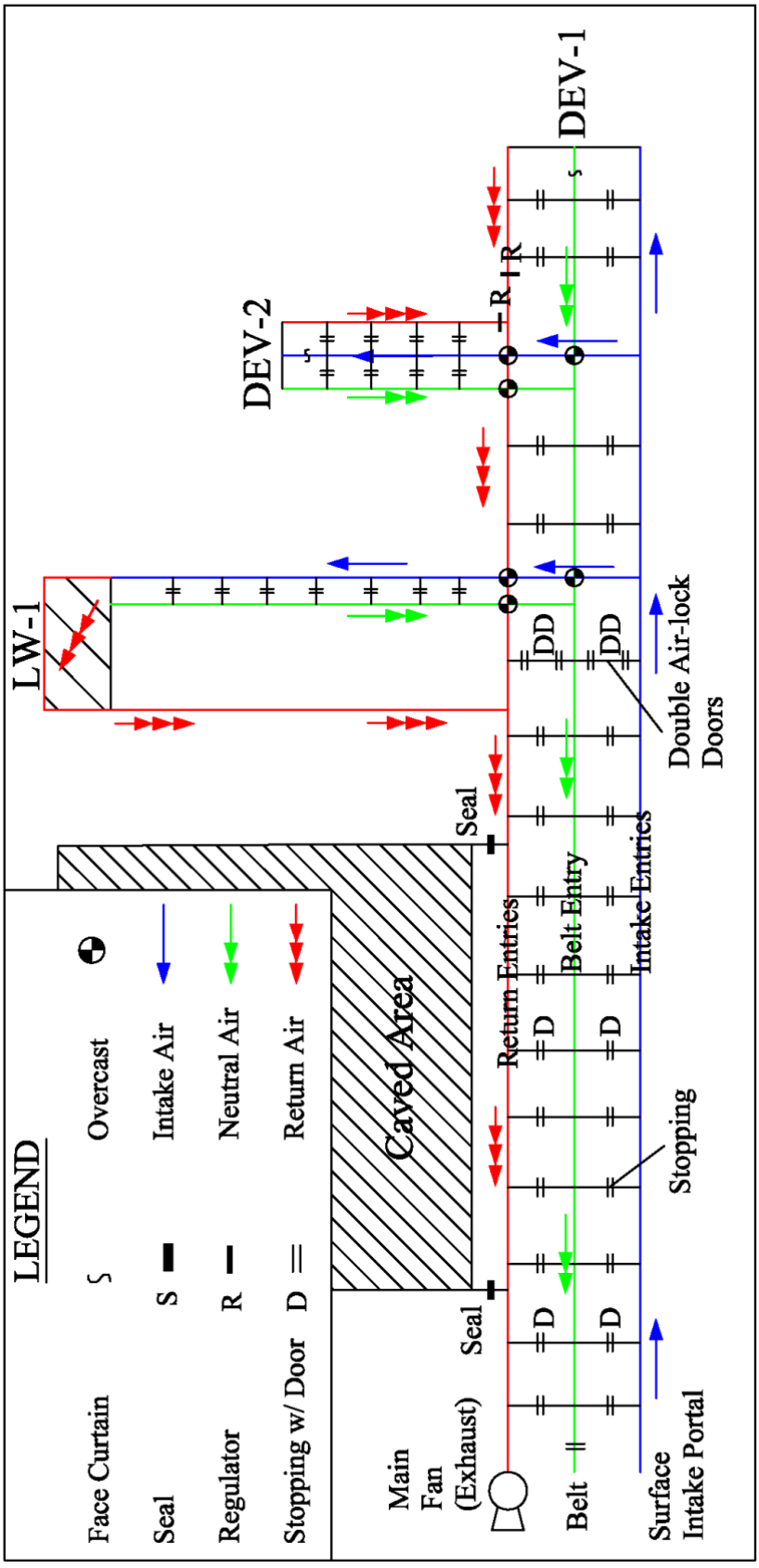

Figure 2.1 A typical coal mine ventilation system with an exhausting main fan

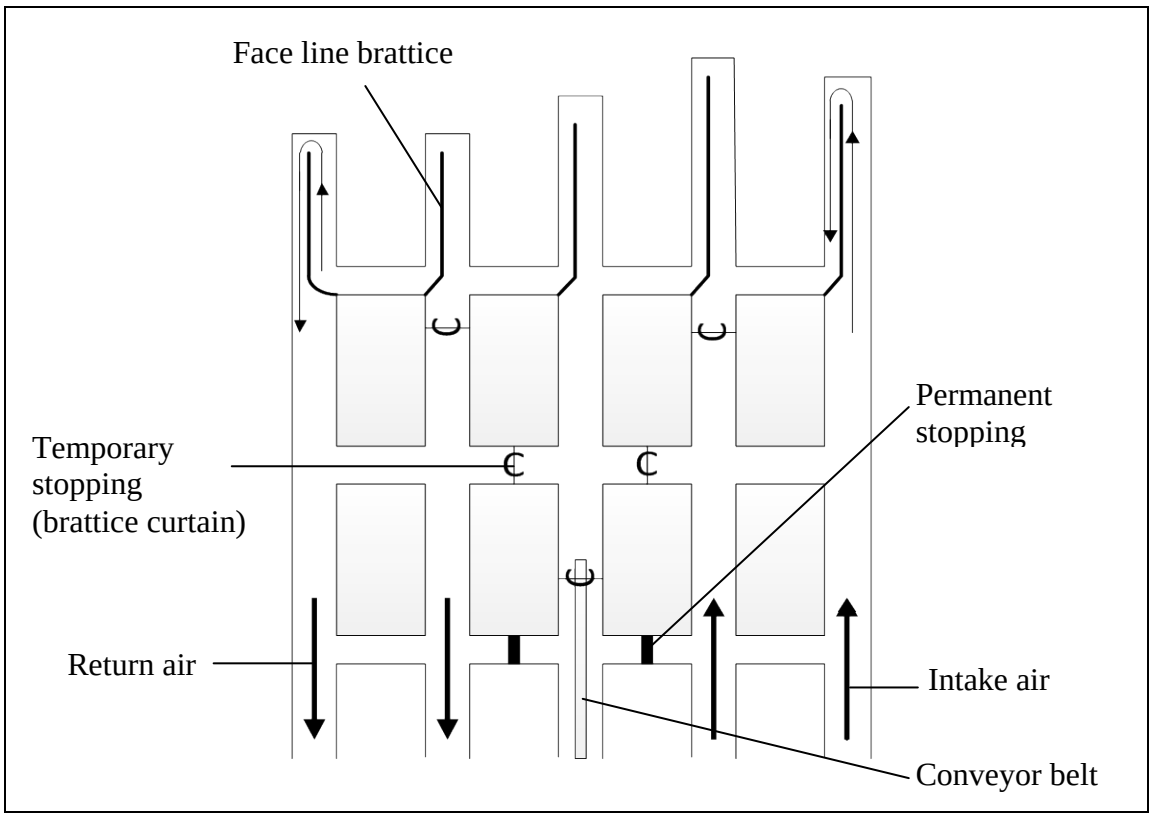

Figure 2.2 Diagram showing face ventilation of a room and pillar development heading

As it passes through the working sections, the air picks up contaminants and is then directed out of the mine through return airways. The return air eventually exits the mine by means of one or more additional connections to the surface. The return air is monitored and regulated so that appropriate actions can be taken to avoid reaching hazardous concentrations of methane or other contaminants.

Finally, most coal mines have a neutral airway. This is the airway where the belts that transport the coal out of the mine are located. The neutral airways are also governed by specific regulations as to provide a safe working environment. In the past, U.S. laws required neutral air to be directed away from the working sections. This regulation was based on the logical assumption that the belt entry is a more likely location for a fire to

ignite. For the protection of the workers, in the event that a fire did ignite, the resulting toxins would not be directed toward the active heading, but would instead be exhausted toward the surface portals.

As mines have expanded over the years, it has become more difficult to properly ventilate the faces. At the same time, more technologically advanced monitoring devices have been developed. As a result, laws have been modified to allow operators to utilize the belt entry as a means to supply additional air to the working sections (30 CFR § 75.350). There is a maximum quantity that is permitted, and this may only be done with the use of an atmospheric monitoring system (AMS). An AMS must include early-fire-detection equipment such as gas detectors (CO, CH_4, O_2), strategically placed video cameras, and heat sensors (30 CFR § 75.351).

2.2 *Mine Fans*

2.2.1 Surface Fans

Main fans create the pressure differential needed to move the air by either blowing or exhausting air through the mine. In a mine with a blower fan, or forced system, the fan blows air into the intake entries. This raises the pressure in the entries above the atmospheric pressure and causes the air to flow toward the return. In an exhausting system, the fan is located in the return and it lowers the air pressure below the atmospheric pressure. This causes the air outside the mine to flow into the intake entries.

A forced system is a *positive* pressure system whereas an exhaust system is a *negative* pressure system. A forced system is primarily advantageous in a condition where gas is inexhaustible. For example, if an active mine is located close to abandoned workings that contain toxic gasses, an exhausting system will continually draw these

gasses through fissures and contaminate the active mine. A forced system will reduce or even eliminate this problem.

In contrast, the most significant advantage of an exhausting system is the continuous reduction of the absolute pressure in the mine by the fan. While the fan is running, gas from the gob, face, or sealed areas is drawn into the return entries where it can be diluted and exhausted. If the fan fails, due to a power outage for example, the pressure in the mine increases and the ventilated portion is at a higher pressure than the sealed or gob areas. As long as the pressure in the active workings is greater than that of the gob areas, gas migration from those areas is impeded.

In a forced system, the active mine area is at an absolute pressure higher than the outside pressure while the fan is running. If the fan stops, the pressure inside the mine decreases, while the sealed areas remain at the higher pressure. This causes gas to begin flowing from the sealed areas to the active workings at the time the fan stops.

Another distinct difference between forced and exhausting systems is that a forced system requires the use of air-lock doors near the entrance of the mine. Properly maintaining air-lock doors is difficult and expensive. In general, exhausting systems have more advantages than forced systems, particularly for coal mines. However, many of the characteristics common to a traditional forced system are really characteristic of the way a forced system is used, and are not really factors related to the fact that the air is forced through the mine (Kennedy, 1996).

Another important factor pertaining to fans is the design of the fan itself. There are two major fan designs: axial and centrifugal (radial). The axial fan has a propeller similar to that of an aircraft, watercraft, or a common desk fan. Air passes through the fan

propeller, along the axis of rotation so the inward and outward flow directions are the same. A centrifugal fan on the other hand, resembles a paddle wheel. Air enters through the center of the wheel along the axis of rotation and exits perpendicular to the axis of rotation by centrifugal action. In both axial and centrifugal designs, the number and position of the blades (spacing, tilt angle, etc.) may be varied to adjust the performance of the fan. Some fans are equipped with pneumatic or hydraulic controls to make these adjustments while others must be changed manually. Manual adjustment can also become impossible if the fan is not serviced routinely. Adjustments in the fan performance can be easily made without adjusting blade position if the fan motor is equipped with a variable frequency drive (VFD), although there are also some limitations to this method as well (Hartman et al., 1997). A significant quantity of air will leak directly through the fan housing if the fans are not carefully and properly installed, including optimizing the layout and engineering design. Numerical modeling should be used to achieve proper and efficient design, installations, and operations to maximize fan energy efficiency (Basu et al., 2004).

2.2.2 Booster Fans

A booster fan is an underground ventilation device installed in the main airstream (intake or return) to handle the quantity of air required for one or more working districts (McPherson, 1993). It is installed to operate in series with a main fan and boost the air pressure of the ventilation air passing through it. To accomplish this objective, the fan is installed in a permanent stopping and equipped with airlock doors and interlocking devices. A monitoring system, equipped with environmental and fan monitors, is used to continuously assess the operating conditions of the fans. Currently in the US, booster fans

are permitted for use in most metal/nonmetal mines. But with the exception of anthracite mines, booster fans are not allowed in coal mines (30 CFR § 75.302). However, booster fans are currently being used in several coal mines located in countries including the United Kingdom, Australia, Poland, India, and others (Calizaya et al., 2010).

2.3 *Mine Ventilation Control Structures*

A ventilation control structure is defined as any device that is used to direct airflow to where it can be usefully employed in the mine. A mine ventilation system is comprised of a wide variety of structures depending on the particular purpose. As a result, over time, a mine ventilation system can become somewhat complex. The mine map shown in Figure 2.1 depicts locations of the most common structures used in coal mines, which include stoppings, stoppings with doors, regulators, air-lock doors, overcasts (air crossings), seals, and face curtains. More detailed descriptions of these common structures are given in the following subsections.

2.3.1 Stopping (bulkhead)

The stopping is by far the most common ventilation structure used in coal mines. A single mine will typically need thousands of stoppings throughout the mine life. A stopping is a wall or barrier erected to direct airflow to the working sections. Depending on its purpose, a stopping can be either temporary or permanent. Usually made of some form of fire-resistant plastic or brattice cloth, temporary stoppings are used in working sections where frequent adjustments to air direction are required. Temporary stoppings are such that they can be installed and removed relatively quickly. Permanent stoppings are placed where long term ventilation control is needed, for example between intake and return entries in a longwall panel, submains and mains. Federal regulations require

permanent stoppings to be maintained up to and including the third connecting crosscut outby the working face (30 CFR Section 775.333(b)(1)). They are intended to be built so as to be airtight and effectively separate two different airways. Permanent stoppings can be constructed using a variety of materials and methods. Some examples include concrete, cinder blocks, steel panels and light-weight cementitious blocks. A common light-weight cementitious-block stopping is shown in Figure 2.3.

2.3.2 Stopping with Door

Permanent stoppings can be built with a movable partition to permit passage of personnel or equipment. *Personnel doors* are usually small (0.3 m^2) openings with a spring-loaded door and latch. A rubber gasket is located on the door perimeter to prevent air leakage, while the door itself is usually made of steel. Examples of personnel doors are shown in Figures 2.4 and 2.5. *Equipment doors* are much more robust and must be

Figure 2.3 Photograph of an Omega block stopping

hitched into the roof, ribs, and floor. They are usually double hinged doors, and may be opened and closed automatically, or manually. An automatic equipment door is shown in Figure 2.6.

2.3.3 Air-lock Doors

Air-lock doors are used when personnel or vehicles must pass through a location having high-pressure differential, or from one airway type to another (i.e., intake to return). They consist of two or more doors installed in series, having enough distance between them to accommodate whatever needs to pass through. Air-lock doors are needed near the main fans whether these are installed as blower or exhaust fans. By definition, air-lock doors are included as part of a booster fan installation design. They are also needed for personnel to pass through the fan housing. The equipment door shown in Figure 2.6 could also be used as an air-lock door.

Figure 2.4 Photograph of an Omega block stopping with a personnel door

Figure 2.5 Kennedy panel stopping with a personnel door

Figure 2.6 Stopping with automatic equipment doors

2.3.4 Regulator

A regulator is a device used to intentionally create shock loss to restrict passage of air through an airway. They are used to regulate the amount of air allowed to flow through a specific section or split. They are usually set in permanent stoppings as adjustable, sliding partitions that can be varied to the desired opening. The stopping shown in Figure 2.7 has a small regulator (closed) as well as a personnel door. Regulators are usually located on the return side of an air split to minimize interference with traffic.

Figure 2.7 Pressure drop being measured across an Omega block stopping with a personnel door and regulator

2.3.5 Overcast

An overcast is a bridge-like device used to permit the crossing of two streams of air at an intersection without allowing them to mix as illustrated in Figure 2.8. It is constructed using the same types of materials as stoppings (concrete or steel) and like stoppings is intended to be airtight. In Figure 2.1, overcasts are required in order to develop the section of longwall gateroads (DEV-2) perpendicular to the mains (DEV-1). Two are needed where the DEV-2 intake airway crosses the belt and return airways of DEV-1 and a third is needed where the DEV-2 belt entry crosses the DEV-1 return airway. In practice, those shown on the map in Figure 2.1 may represent multiple structures and they are often equipped with mandoors for convenient access.

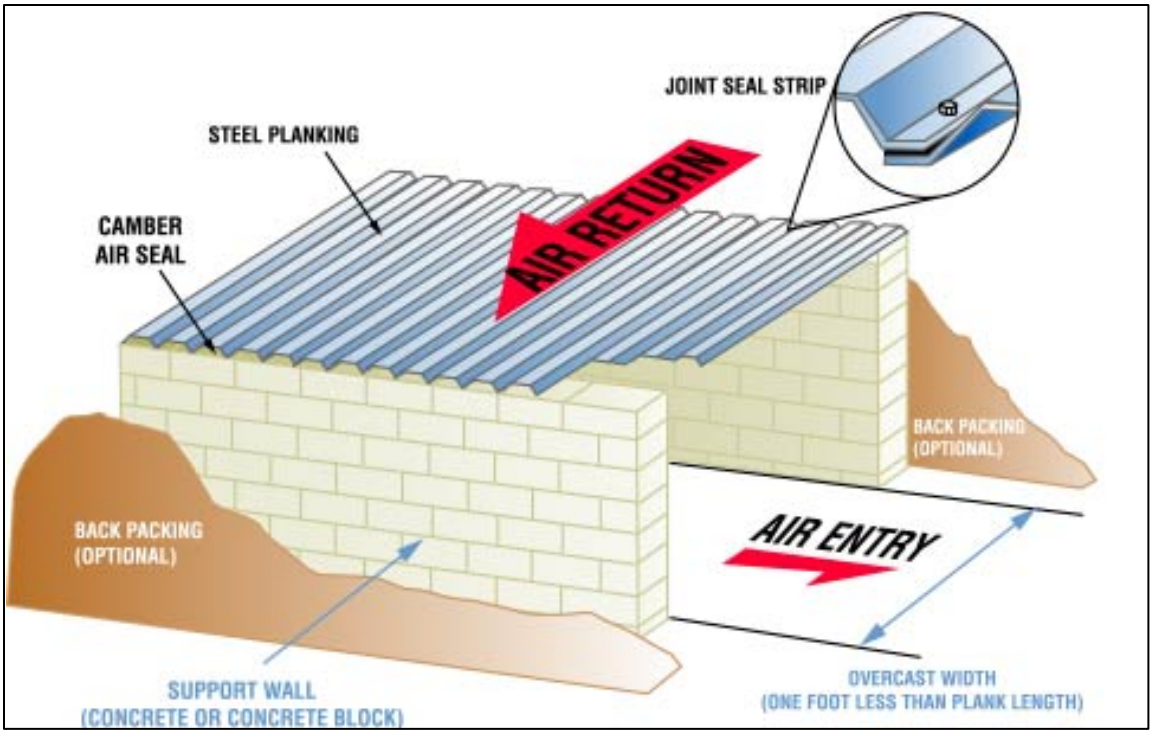

Figure 2.8 An overcast constructed using Camber Steel Planks Overcast Tops bolted to the top of cinder block walls (from Camber Corporation: www.cambergroup.com/mine.htm)

2.3.6 Seal

A seal is a special type of stopping used to isolate abandoned workings. As the name suggests, a seal is intended to completely isolate an area from the active mine workings. As such, it is required to be very robust as to withstand the pressures inside the mine, including potential explosions on either the abandoned side or working side. There are two general types of seals: gob seals and mine seals. Gob seals are those used to isolate an abandoned section of the mine such as the caved area in Figure 2.1, whereas mine seals are used to seal the mine portals at the end of the mine life. An example gob seal is shown in Figure 2.9.

In the past, common practice in the case of gob seals was to construct a solid-block, permanent stopping having twice the thickness of a regular solid-block stopping

Figure 2.9 Gob seal constructed with steel Kennedy panels and Omega blocks

(Stephan, 1990; Sawyer, 1992). One or more pilasters were also installed in the center of the seal to add structural integrity. However, following the 2006 Sago mine explosion in which 10 seals were destroyed (Federal Register, 2007), the MINER Act of 2006 called for seal design requirements to be improved. Each individual seal must now have a site-specific design, be professionally engineered to meet minimum overpressure standards, and be approved by the US Mine Safety and Health Administration (MSHA) prior to being installed in a mine (Zipf et al., 2007).

Mine seals, on the other hand, are typically composed of two concrete or masonry block gob seals constructed some distance apart, with a fill material placed between them. The fill material may be concrete, earth, or a combination of other materials. Recently there have been some concerns regarding the adequacy and safety of mine seals as well. Researchers are currently developing guidelines for adequate designs (M.G. Nelson, personal communication).

2.3.7 Brattice Cloth Face Curtain

A face curtain is a fire resistant plastic or cloth curtain that is hung longitudinally in a dead-end heading. It divides the entry in two so that air is directed to the face along one side of the brattice and returned along the other side. Brattice curtains are also used as temporary stoppings as shown in Figure 2.10, until a permanent one can be installed.

2.3.8 Auxiliary Fans and Ventilation Tubing

An auxiliary fan in conjunction with ventilation tubing is used to either supply or remove air from a working face, using an additional duct for airflow. The use of fans and vent tubes in coal mining is an alternative to the use of curtains for ventilating dead ends in an active development section. The auxiliary fan must be properly sized to supply the

required quantity of air to the face, and installed in such a way as to prevent recirculation. If the auxiliary fan is turned off, face curtains must be used.

Figure 2.10 A brattice cloth curtain installed as a temporary stopping with polyurethane foam sealant applied along the perimeter for air tightness (from Strata Products International, 2010)

3 MINE VENTILATION FORMULAE

Air flow in mine ventilation is an example of a steady fluid flow process, (none of the variables of flow changes with time), with transitions and losses in energy. Detailed descriptions of fluid flow theory applicable to underground mining are found in mine ventilation textbooks (Hall, 1981; McPherson, 1993; Hartman et al., 1997). The basic principles and assumptions used in subsurface ventilation are given in this chapter.

3.1 *Fluid Flow Principles*

Air is a mixture of gases and water vapor, and is compressible. However, if the mass density is nearly constant, it can be considered an ideal, incompressible gas. This condition exists in most mine ventilation situations. Exceptions to this include mines that require significant heating or cooling, as well as those that have vertical air movements in excess of 500 m (1,640 ft). In these situations, thermodynamic laws must be applied. Since the heat energy is neglected, the total energy at any section in a moving fluid (in this case air) consists of the sum of static (p/γ), velocity ($V^2/2g$), and potential (Z) energies. This is shown in the well-known Bernoulli equation for incompressible gases:

$$\left(\frac{p_1}{\gamma}\right) + \left(\frac{V_1^2}{2g}\right) + Z_1 = \left(\frac{p_2}{\gamma}\right) + \left(\frac{V_2^2}{2g}\right) + Z_2 + H_L \qquad (3.1)$$

where

p = absolute air pressure (Pa)

V = air velocity (m/s)

γ = specific weight of the air (kg/m^3)

Z = measuring point elevation (m)

H_L = head loss (m)

The subscripts 1 and 2 denote any two individual measurement locations. In practice, it is convenient to make all head measurements on a gage-pressure basis:

$$H_s = p / \gamma \tag{3.2}$$

$$H_v = V^2 / 2g \tag{3.3}$$

where

H_s = static head (m)

H_v = velocity head (m)

When this is done, the measuring point elevations (Z) are omitted, and Equation 3.1 can be written as:

$$H_{s1} + H_{v1} = H_{s2} + H_{v2} + H_L \tag{3.4}$$

This is called the modified energy equation. At any point in the system, the total head H_t (m) is the sum of velocity and static head:

$$H_t = H_s + H_v \tag{3.5}$$

Pressure (Pa) measurements are obtained by multiplying the head values in Equation 3.5 by the specific weight of air, giving:

$$p_t = p_s + p_v \tag{3.6}$$

The energy losses in a mine are illustrated by considering the pressure gradient of a simple system.

3.1.1 Mine Pressure Loss

Consider airflow through a duct having three sections: (a), (b), and (c). Figure 3.1 shows a blower fan at the inlet of Section (a), an expansion between Sections (a) and (b), a contraction between Sections (b) and (c), and a discharge at the end of Section (c).

The fan creates a pressure difference between the inlet and outlet that is consumed in overcoming flow energy losses. The figure shows a large initial pressure increase induced by the fan followed by a gradual reduction in pressure through (a). There is a rapid decrease in velocity head at the pipe expansion at (a) to (b), followed by another gradual loss through (b). The pipe contraction from (b) to (c) causes another abrupt change in velocity head followed by another gradual decrease through (c). The mine static head, mine $H_{s,}$ includes all of the pressure head losses that occur along the airstream between the inlet and outlet. These head losses are made up of two components, frictional loss H_f caused by the resistance of the walls on the airstream, and shock loss H_x, caused by abrupt changes in the airstream velocity:

$$\text{mine } Hs = \Sigma H_L = \Sigma (H_f + H_x) \tag{3.7}$$

Notice that the inlet velocity head is negative. This occurs because a suction condition must exist here in order for air to flow into the system. Similarly, the discharge velocity head is positive because the air is in motion when it leaves the system and is lost to the system in the form of kinetic energy. The loss of velocity head at the discharge is minimized by converting some of it to static head through the use of a diffuser duct or

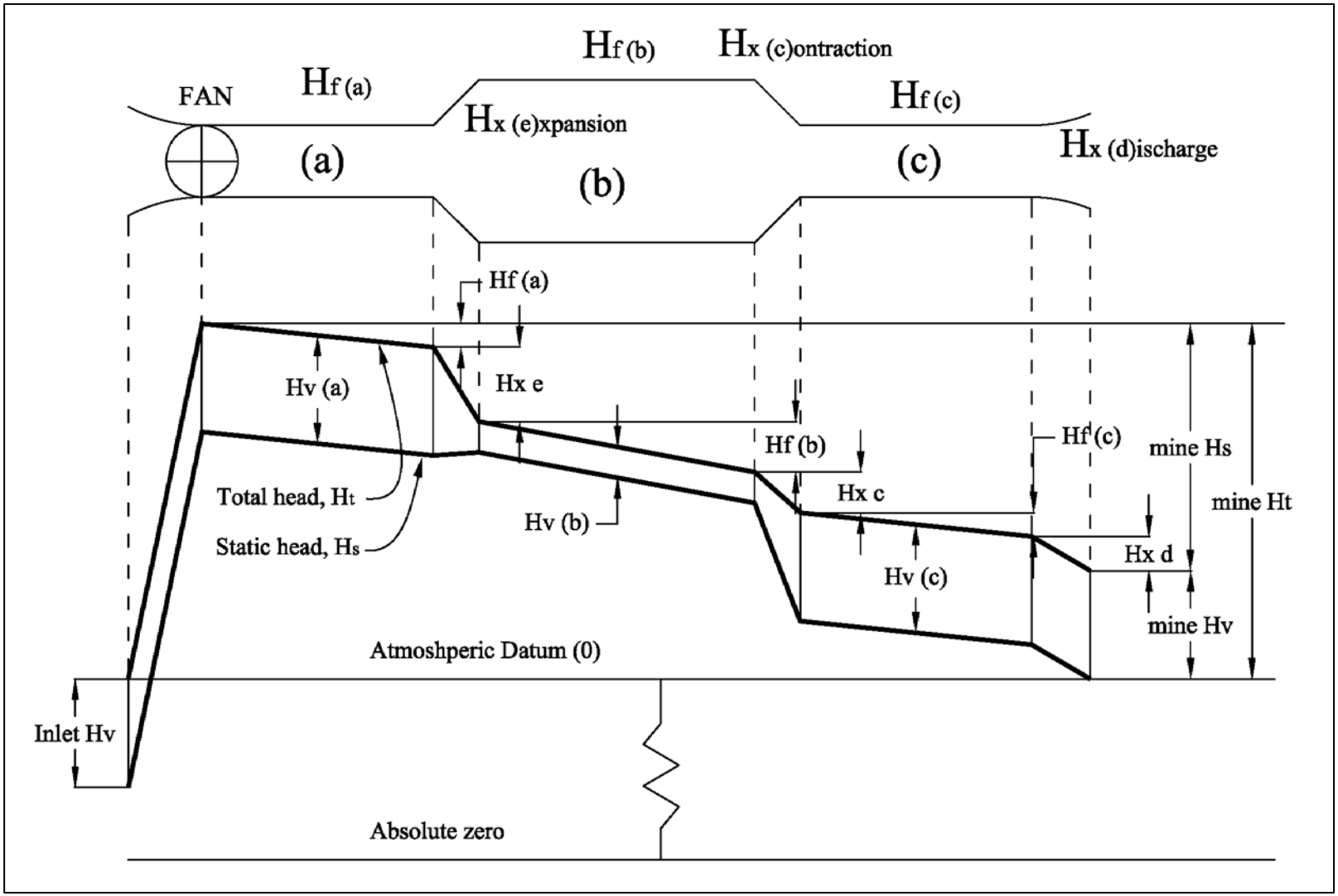

Figure 3.1 An example ventilation system with a blower fan to demonstrate pressure losses in a mine

evasé discharge, a standard practice in mine ventilation.

3.1.2 State of Airflow

In fluid mechanics, two distinct states of fluid flow are defined: laminar and turbulent. It is necessary to identify the state of flow that prevails because the fluid behaves differently in each state. The criterion used in establishing boundaries for each state is the dimensionless Reynolds Number N_R. Laminar flow exists where $N_R < 2000$ and turbulent flow where $N_R > 4000$. The region between is known as the intermediate range. For any fluid flow conditions, the N_R can be determined from measurements and fluid properties:

$$N_R = \frac{\rho DV}{\mu} = \frac{DV}{\nu} \tag{3.8}$$

where

N_R = Reynolds Number (dimensionless)

ρ = density of the fluid (kg/m^3)

V = relative velocity of the fluid (m/s)

D = diameter of conduit (m)

μ = dynamic viscosity (Pa·s)

ν = kinematic viscosity (m^2/s)

In mine airways, it is important that turbulent flow always prevails to provide sufficient dispersion and removal of contaminants (Kennedy, 1996). Using typical dimensions of mine openings and air velocities in Equation 3.8, it is evident that turbulent flow will nearly always prevail in any mine airway. Exceptions to this include laminar

flow in caved areas and "air-tight" stoppings (Hartman et al., 1997). The state of airflow in a mine can also be perceived in terms of resistance to airflow.

3.2 *Mine Resistance to Airflow*

Turbulent flow prevails in mine airways that have relatively low resistance to flow, whereas laminar or semilaminar flow is found in areas that have high resistance such as gob areas and ventilation control structures. Resistance in these locations is typically several orders of magnitude higher than in most mine airways.

3.2.1 Airway Resistance

The friction losses typically constitute 70 to 90% of the total losses (Hartman et al., 1997). Friction losses are caused by the drag forces between the walls and the air streams, which depend primarily on the roughness of the individual wall surfaces. For example, moving air through a smooth duct requires less horsepower than moving air through the same size duct with rough walls. Thus, rough walls have higher frictional resistance to flow.

Shock losses are caused by abrupt changes in air velocity and can be determined directly by the following equation:

$$H_x = X \cdot H_v \tag{3.9}$$

where

H_x = shock loss (Pa)

X = shock loss factor (dimensionless)

Obstructions in the airstream include changes in direction (such as a 90° turn) as well as changes in the size of the opening (inlet, discharge, regulators). Although shock

losses constitute only 10 to 30% of the total head loss in mine ventilation systems, an attempt should be made to avoid conditions that cause unnecessary shock losses. Corners should be rounded and acute angles in the entryways should be avoided if possible.

The resistance of an airway can be determined and quantified so entries or shafts can be compared and the ventilation performance predicted. This is done using Atkinson's Equation for mine ventilation.

3.2.2 Atkinson's Equation for Mine Ventilation ("The Square Law")

In 1854 J.J. Atkinson published an equation that was originally derived from the Chezy-Darcy fluid flow equation. Atkinson's Equation is applicable to incompressible fluid flow that is turbulent in nature. As such, it is perhaps the most widely used equation in mine ventilation:

$$\Delta p = \left(\frac{k \cdot L \cdot O \cdot V^2}{A}\right) \tag{3.10}$$

where

Δp = differential pressure (Pa)

L = length (m)

O = perimeter of the mine entry (m)

V = average velocity (m/s)

A = cross-sectional area (m^2)

k = friction coefficient (kg/m^3, a function of density)

The parameters in Equation 3.10 are average values and/or differential measurements between two locations. In mines, airflow quantities are calculated from measurements of velocity and cross-sectional area of an airway:

$$Q = V \cdot A \tag{3.11}$$

where

Q = airflow quantity (m^3/s)

By replacing V with Q/A, Equation 3.10 can be written as:

$$\Delta p = \left(\frac{k \cdot L \cdot O}{A^3}\right) \times Q^2 \tag{3.12}$$

If air density remains constant between the two measurement points, then k, L, O and A are all known values and collectively make up what is termed the resistance value, R. Thus, Equation 3.12 can be simplified to what is commonly called the Square Law of mine ventilation.

$$\Delta p = R \cdot Q^2 \tag{3.13}$$

where

R = airway's resistance value (Ns^2/m^8)

Equation 3.12 quantifies only the friction losses, not shock losses. In practice shock losses are usually expressed as an equivalent length L_e. By doing this shock losses can easily be adapted into Equation 3.13:

$$\Delta p = \left(\frac{k \cdot (L + L_e) \cdot O}{A^3}\right) \times Q^2 \tag{3.14}$$

The equivalent length is still a function of the shock loss factor. Calculating the shock loss factor is time consuming. Therefore common values of shock loss factors and equivalent lengths in ventilation designs given in textbooks are used (Hartman et al., 1997; McPherson, 1993).

3.2.3 Friction Factors

Pioneering work concerning friction factors in mines was published in 1935 by the U.S. Bureau of Mines (McElroy) based on experimentation conducted primarily in metal mines. These values have been widely accepted for application to both metal and coal mines not only in the past but also in recent years (Francart and Wu, 2002).

In 1974 results of an extensive study regarding leakage and friction factors in coal mines was published (Kharkar et al., 1974). The researchers evaluated six eastern U.S. coal mines with varying conditions of roadways and stoppings. One important conclusion of the study was that there was a general decrease in the value of friction factors as compared with McElroy's 1935 values.

Since the 1970s, there have been numerous publications in which friction factors are given. Several of these are textbooks which suggest using McElroy's original 1935 values (Hall, 1981; Hartman et al., 1997). There have also been various publications of friction factors based on personal experience or empirical formulae (Bruce and Koenning, 1987; McPherson, 1993; Duckworth et al., 1995; Richardson et al., 1997). Engineers at Mine Ventilation Services, Inc. (MVS) have collected data over the course of 15 years and made a comparison between textbook values and their own measured values (Prosser and Wallace, 1999). The comparison shows that recently published friction factors for coal mines are consistent with those published earlier by both Kharkar et al. (1974) and

McPherson (1993). The comparison further found that the MVS values are consistently lower than the values quoted in textbooks. In fact, MVS did not measure a single friction factor as high as those given by McElroy in 1935.

This discrepancy has been attributed to the evolution of modern mining techniques. Modern mining methods use bigger and more systematic mechanized equipment. This results in mines having smoother, larger and more regularly shaped airways which in turn have lower friction factors. A summary of common friction factors is located in Table A.1 of Appendix A. A summary of common resistance values is located in Table A.2.

3.2.4 Multiple Airways

All of the principles thus far presented are applicable only to singular airways. Ventilation circuits can be described by the fundamental laws governing the behavior of electrical circuits in series and parallel (Kirchhoff's first and second laws). Kirchhoff's first law states that the flow entering a junction equals the flow leaving that junction. For air, this is mass flow, for electricity, this is current. If the variation in air density around any single junction is negligible in the mine ventilation system then the algebraic sum of the volume flow rates entering and leaving each junction equals zero. The simplest statement of Kirchhoff's second law applied to ventilation networks is: the algebraic sum of pressure drops along any closed circuit equals zero.

Therefore, the equivalent resistance R_e for n number of mine airway sections in series is calculated by:

$$R_e = R_1 + R_2 + ...+ R_n \tag{3.15}$$

Similarly, an equivalent resistance R_e for n number of airways in parallel can be determined by:

$$\frac{1}{\sqrt{R_e}} = \frac{1}{\sqrt{R_1}} + \frac{1}{\sqrt{R_2}} + \cdots \frac{1}{\sqrt{R_n}} \tag{3.16}$$

In the case of coal mines, similar characteristics are often encountered in the various portions of the ventilation system. That is, entries in a particular mine are typically driven at the same width and height and with the same equipment (a continuous miner unit). If the airways have similar conditions and characteristics (k-factor and physical dimensions), then the resistances of all the airways are the same and Equation 3.16 is more usefully written as:

$$R_e = R_i / N_a^2 \tag{3.17}$$

where

R_i = resistance of a single airway (Ns^2/m^8)

N_a = the number of parallel airways

Equation 3.17 demonstrates that as the mine workings expand, the resistance of a single airway quickly becomes too great for the fan power to overcome. Thus, a practical method to reduce airway resistance and supply a higher air quantity is to develop parallel entries.

3.2.5 Leakage Path Resistance

The connecting crosscuts between entries are developed in the same manner as in the main entries. Therefore, prior to having stoppings installed, the crosscuts have the

same characteristics (i.e., resistance) as airways. Once the stoppings are installed, common practice is to simply treat crosscuts with stoppings as airways having very high resistance. In this way, the Square Law can be applied and if the pressure differential and quantity are measured, the stopping resistance can be calculated using Equation 3.13. The main problem encountered with this method is the high level of variability in field measurements.

Bruce and Koening (1987) reported measured resistances for individual masonry stoppings, in good condition, ranging from 559 to 781,900 Ns^2/m^8, and 1 to 112 Ns^2/m^8 if the stopping had experienced some deformation or was poorly constructed. These values are for stoppings with dimensions of 6.1 m (20 ft) by 2.1 m (7 ft). In 2008, Oswald reported a range of stopping resistances based on type of material and condition, but not dimensions. These values range from 1,786 to 6,628 Ns^2/m^8 for Kennedy stoppings and 2,425 to 10,674 Ns^2/m^8 for concrete block stoppings. In their study, the average resistance for new, "ideally constructed," concrete block stoppings, is 51,696 Ns^2/m^8. A continued effort to classify resistance based on criteria such as physical dimensions, porosity, and age-based conditions will help refine future reported resistances.

3.3 *Leakage Flow*

There is a consensus in the mining industry that air leakage is a major problem in mine ventilation systems. However, there has been some disagreement as to how the leakage paths and leakage distribution are characterized.

In 1942 Mancha addressed the effect of leakage through stoppings on mine fan performance. An effort was made to characterize the distribution of air leakage in a simple mine ventilation circuit and it was suggested that the percent of circuit pressure

increase results in a proportional increase in percent leakage. Mancha (1942) further suggests that a lack of empirical data and knowledge of the condition of individual stoppings makes an exact analysis of leakage through stoppings underground impossible. This idea may be true, but reasonable efforts have been made.

Leakage flow is defined as any quantity of air that is not usefully employed somewhere in the mine. This quantity can be determined indirectly:

$$Q_L = Q_T - \sum Q_E \tag{3.18}$$

where

Q_L = leakage quantity (m^3/s)

Q_T = total air quantity at the fan (m^3/s)

Q_E = air quantity reaching a working area (m^3/s)

A working area is any location that requires a minimum flow quantity. Examples include longwall (LW) and continuous miner (CM) sections, pumping stations, underground shops, charging stations, bleeder monitoring points and gob seals.

The total percent leakage in the system is the ratio of the quantity of air that is short circuited before reaching the working areas to the total quantity circulated by the fan. It is calculated as follows:

$$L_T = (100) \cdot (Q_T - \sum Q_E) / Q_T \tag{3.19}$$

where

L_T = total leakage (%)

If the cross-sectional area remains constant throughout the system, for convenience, the average velocity can be used to calculate the total leakage:

$$L_T = (100) \cdot (V_T - \sum V_E) / V_T \quad (3.20)$$

where

V_T = average velocity at the fan (m/s)

V_E = average velocity at the working section (m/s)

3.3.1 Methods of Estimating Leakage Through Stoppings

There are two standard methods of measuring leakage quantity through stoppings. This can be done directly through individual stoppings, or indirectly through multiple stoppings.

Leakage through an individual structure can be accurately measured under a controlled environment (Vinson et al., 1977; Singh et al., 1999). One such technique was developed by the former United States Bureau of Mines (USBM) where the leakage through an individual stopping can be measured using a temporary brattice cloth with a small orifice (Vinson et al., 1977; Weiss, 1993). An example of this method is shown in Figure 3.2. The brattice is installed on the low pressure side of the stopping. The air leaking through the stopping passes through the small orifice, where it is easy to measure. The pressure difference across the stopping is also measured. Using Equation 3.13, the resistance of that particular structure can be quantified.

While measurement methods for individual stoppings may be useful for scientific studies, the processes are time consuming and costly. Furthermore, the leakage of a single structure has been found to be insignificant in comparison to the ventilation system as a whole (provided the structure is in fair condition, having no excessive or unusual damage). As previously stated, the resistances of individual stoppings vary greatly, so it is inaccurate to assume an average resistance for all stoppings based on a single

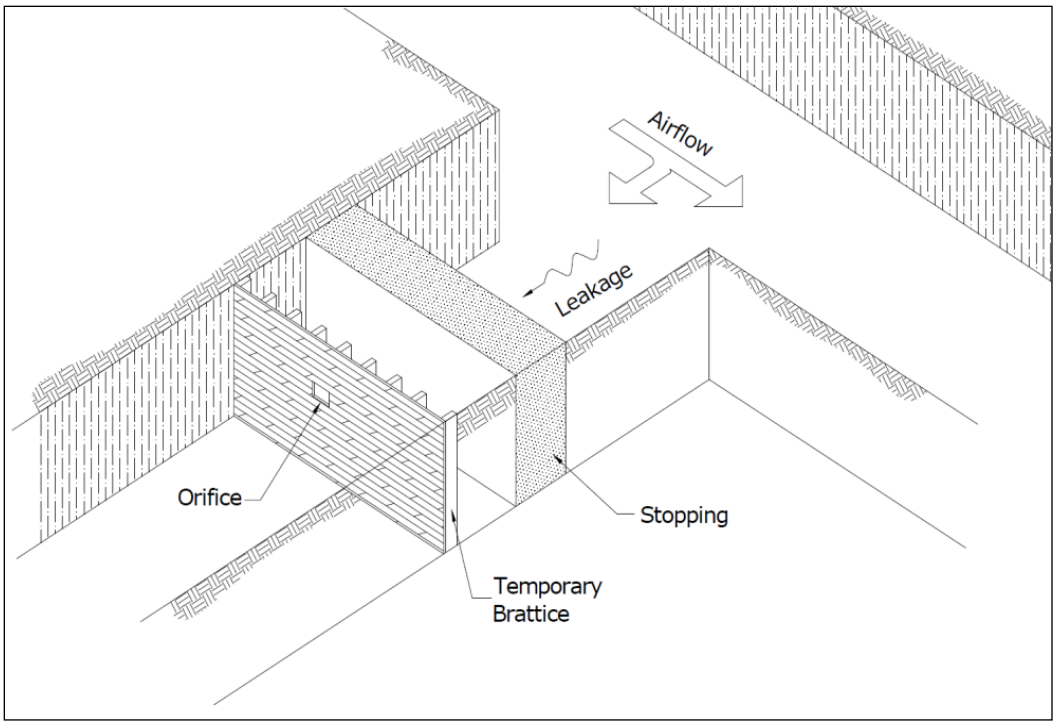

Figure 3.2 USBM method of measuring single stopping leakage and resistance (After Vinson, 1977; from Oswald, 2008)

measurement. A large number of measurements are needed, so it is not practical to measure the leakage through each individual structure.

The other method is to measure the average leakage through a group of stoppings. This method is illustrated in Figure 3.3, which depicts a cut out of a coal mine section having 5 entries. Entries 1 and 2 have intake air, Entries 4 and 5 have return air, and Entry 3 has neutral air. The air courses are separated by stopping lines which periodically contain doors. Entry 3 has systematic box-check regulators to limit the neutral airflow quantity. The total intake flow is the combined measurements in Entries 1 and 2. If airflow measurements are made at section points A and B in the intake air course, the difference between A and B is the amount of intake air leaking through five stoppings into Entry 3. Pressure differentials between Entries 2 and 3 can easily be measured at the

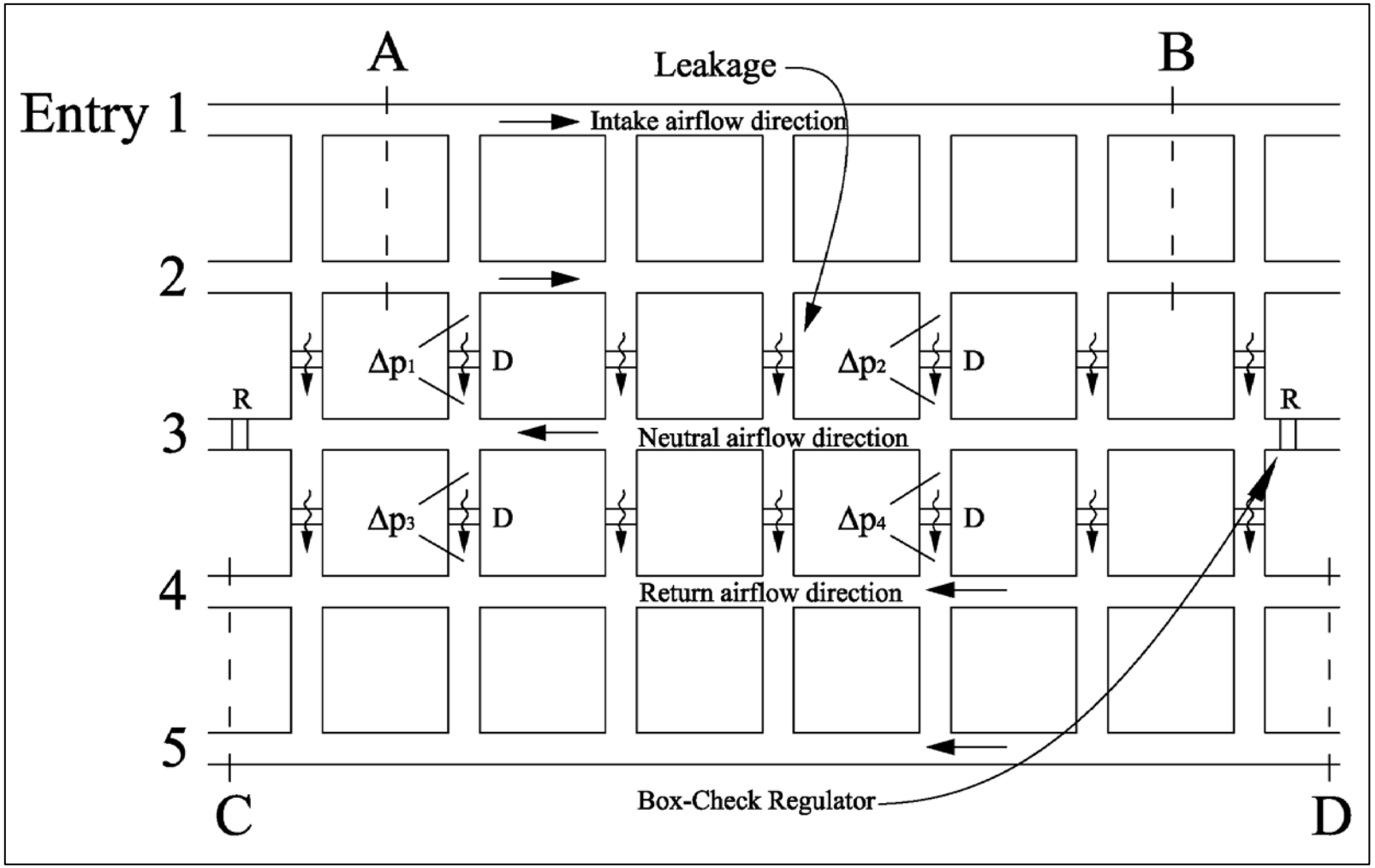

Figure 3.3 Standard method of measuring average stopping leakage and resistance

stoppings containing doors, yielding the average pressure differential across these five stoppings.

If the same method is used on the return side between points C and D the measurements yield the leakage through 7 stoppings. In both cases, Equation 3.13 can be used to quantify an equivalent resistance for the number of stoppings, and the individual stopping resistance is calculated using Equation 3.17 where N_a is 5 for the intake side stoppings and 7 for the return side.

Using this method assumes that the leakage quantities through all the stoppings in a particular group Q_i, are equal ($Q_i = Q / N_a$) which is not necessarily the case. For example, stoppings with doors generally allow greater leakage than those without. This assumption may be valid over short intervals where the differential pressure across the stoppings does not vary significantly, but it is not justified over longer intervals with high variance in differential pressures. This method is not intended to distinguish resistances between individual stoppings, but rather to determine an average resistance for a group of stoppings. The preferred interval is different for each mine and depends on the pillar dimensions, as well as stopping characteristics. This method provides the ability to measure resistance throughout a large mine relatively quickly while still being able to distinguish between groups of stoppings differing in age, condition, and type.

4 COAL MINE FIELD SURVEYS

Ventilation surveys were conducted in two western US underground coal mines. The main objective is to gather data in a real world setting, compare these data with previously published measurements in the literature, and use them to develop a laboratory model with which leakage paths (stoppings, overcasts, doors, regulators, etc) are characterized. The survey techniques used were as described by Prosser and Loomis (2004).

4.1 *Survey of Mine A*

4.1.1 Mine Description

Mine A is a nongassy, room and pillar mine that has three surface portals: one intake, one belt and one return. At the belt entry portal, there is a stopping built around the belt structure to help prevent air from entering the mine at that location. The belt air is maintained neutral throughout the workings. A schematic of Mine A is shown in Figure 4.1. The three air courses run parallel from the portals to the two working sections: Face A and Face B, both of which are CM sections. The lateral development of the mine extends approximately 1.2 km from the portals to Face A.

The ventilation system is powered by a 149 kW axial exhaust fan. This fan is equipped with a variable frequency drive (VFD) motor which allows the fan speed to be set between 500 and 900 rpm. When the fan is set at its highest speed, it can exhaust up to 94 m^3/s of air at 1,200 Pa of static pressure.

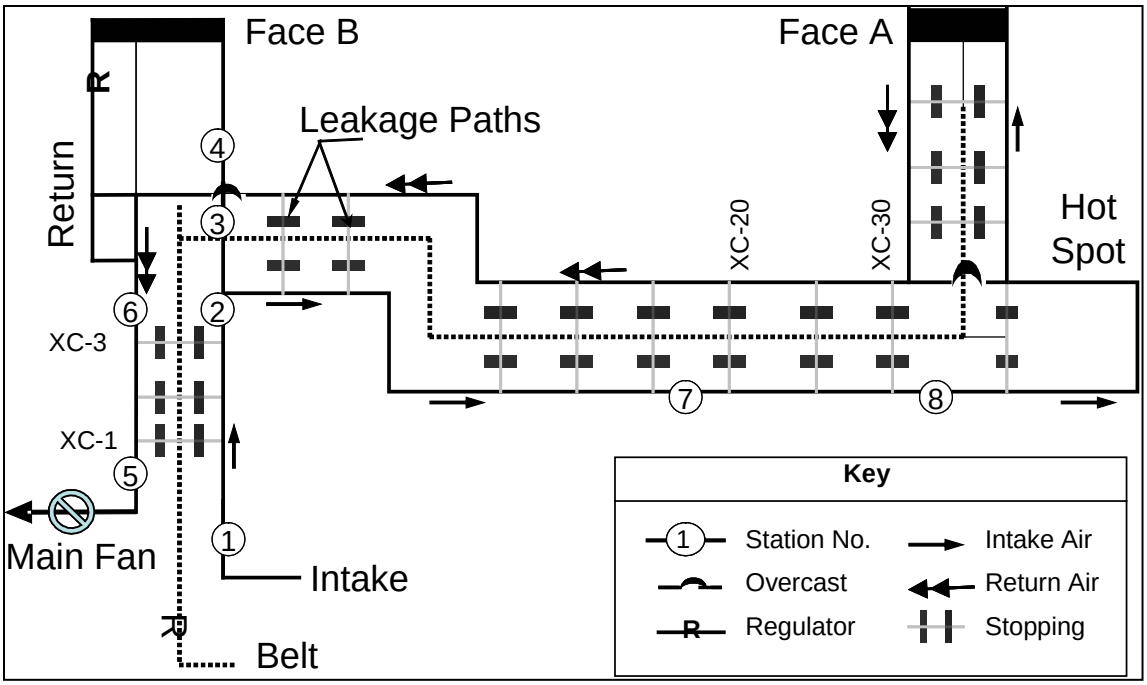

Figure 4.1 Mine A ventilation schematic

The belt entry is located between the intake and return entries and the mine is ventilated using a standard U-type ventilation system in which the belt entries are isolated between the other two, in this case exclusively with Omega-block stoppings. The number of parallel intake entries ranges from one starting at the portal to as many as nine (where rooms are used for storing supplies). However two entries is the most common configuration throughout the mine. The belt air course also typically has two parallel entries, and the return air course has two entries for approximately half the distance between the fan and Face A and only one entry for the remaining half.

Ventilation surveys in this mine were conducted under two conditions: (1) normal fan speed of 500 rpm, at which the fan exhausted 60.46 m^3/s of air at 500 Pa of static pressure, and (2) maximum fan speed of 900 rpm when the fan duty increased to 94.00 m^3/s of air at 1,200 Pa of static pressure. During Condition 1, pressure-quantity measurements were collected from main intake and return airways located near the

surface (between Stations 1 and 6 in Figure 4.1). During Condition 2, the measurements were expanded to monitor the losses of fresh air near Section A (between Stations 7 and 8 in Figure 4.1). In both cases the main objective was to determine the leakage path resistances.

4.1.2 Measurements and Analysis

Table 4.1 shows a summary of air quantity measurements taken from the intake and return entries and the pressure differences across a selected number of stoppings.

This analysis is restricted to leakage path resistances estimated from pressure and quantity (P-Q) measurements shown in Table 4.1. In this case, a leakage path is represented by a set of parallel stoppings installed in cross-cuts adjacent to the belt line. They are used to isolate the conveyor belt line from both the intake and return entries. The analysis is restricted to two sections: Main Return and Southeast Mains. The Main Return section (between Stations 5 and 6 in Figure 4.1) includes three crosscuts (1 through 3). Due to their proximity to the main fan, these stoppings are subject to high pressure differentials. The Southeast Main section (between Stations 7 and 9) includes 10 crosscuts (20 through 30) also blocked by Omega stoppings.

Applying Equations 3.13 and 3.17 to the Mine A measurements yields the following leakage path resistances:

Main Return section (crosscut 1 through crosscut 3):

Condition 1: $R_e = 14.44\ Ns^2/m^8$, and for $N_a = 3$, $R_i = 130\ Ns^2/m^8$.

Condition 2: $R_e = 12.40\ Ns^2/m^8$, and for $N_a = 3$, $R_i = 112\ Ns^2/m^8$.

Southeast Main section (between stations 7 and 8):

Condition 2: $R_e = 3.20\ Ns^2/m^8$, and for $N_a = 10$, $R_i = 320\ Ns^2/m^8$.

TABLE 4.1 Leakage path survey data for Mine A*

Item	Measurement/Location	Condition 1 (500 rpm)	Condition 2 (900 rpm)
1- Fan Duty			
	Quantity, m^3/s	60.65	94.00
	Total head, Pa	498	784
	Pressure across explosion door, Pa	324	560
2- Airflow Rates, m^3/s			
	Intake 1 (portal)	49.13	68.79
	Main intake, Station 2	46.62	na†
	Main intake, Station 3	14.93	23.22
	Main intake, Station 4	10.94	17.01
	SE main intake, Station 7	na	47.06
	SE main intake, Station 8	29.33	43.57
	Main return, Station 5	51.63	80.29
	Main return, Station 6	48.22	74.54
3- Gage Pressure Across Stoppings, Pa			
	Belt to return crosscut 1	187	423
	Belt to return crosscut 3	149	398
	Intake to belt, crosscut 20	na	44
	Intake to belt, crosscut 30	na	34
4- Resistance Per Stopping, Ns^2/m^8			
	Belt to return (Main return)	130	112
	Intake to belt (SE main section)	na	320

*air density = 0.91 kg/m^3.
†na = no measurement.

4.2 *Survey of Mine B*

4.2.1 Mine Description

At Mine B, the coal seam is relatively flat with an average thickness of 4.1 m (13.5 ft). The mine has one longwall (LW) unit and two CM units. The mine workings span nearly 22.5 km (14 mi) from the access portal to the furthest working face. A schematic of Mine B is shown in Figure 4.2.

Dust is the major air contaminant in this mine. The ventilation system is powered by an exhaust fan, which is centrally located with respect to the workings. This is a 3 m (10 ft) diameter axial fan, equipped with a 950 kW (1,275 hp) motor, capable of

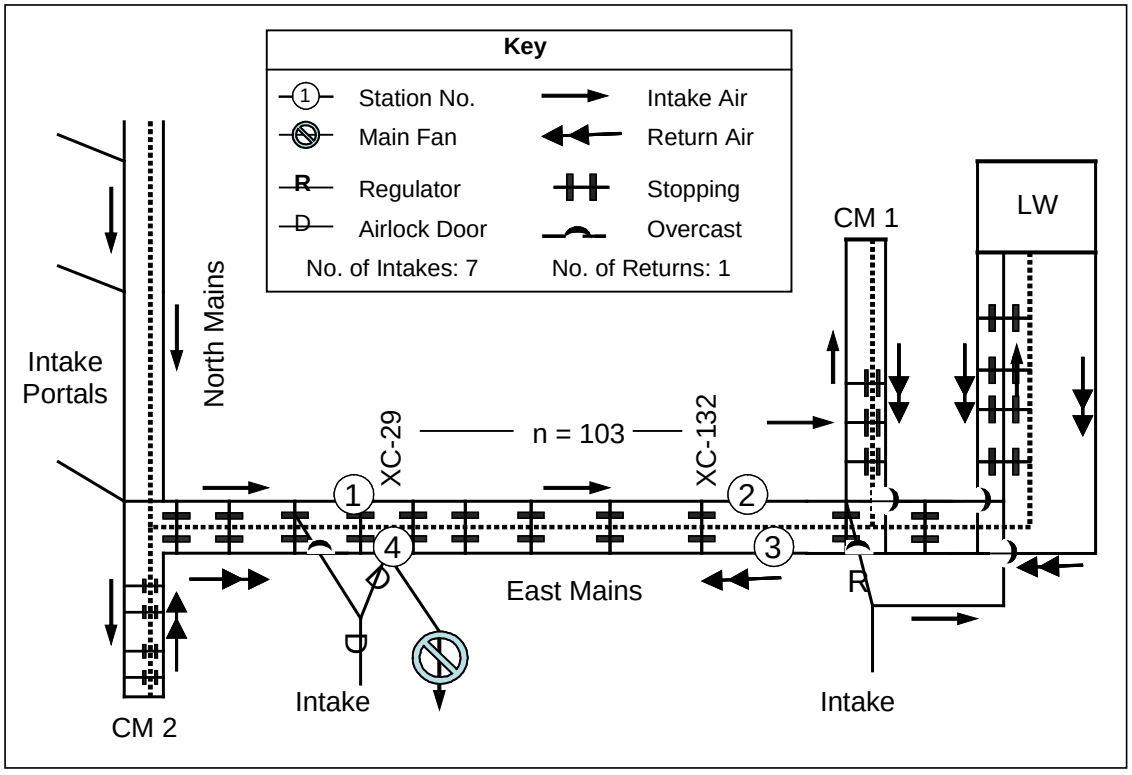

Figure 4.2 Mine B ventilation schematic

exhausting up to 440 m^3/s (930 kcfm) of air at 2,488 Pa (10 in. w.g.). Of the seven intake portals, the one located nearest to the longwall workings provides about 40% of the total air flowing into the mine. A flow-through ventilating method is used wherever possible and the U-type method is used otherwise. Concrete and cinder block stoppings are typically used in the main entries near the fan, while Kennedy stoppings are used in the longwall gateroads. As with Mine A, the main objective was to measure leakage flow rates and pressure losses to determine resistances for stoppings.

4.2.2 Measurements and Analysis

Table 4.2 is a summary of P-Q measurements collected from this mine. The measurements are divided into three sets: one set to determine the overall efficiency of the system, and two sets to determine the leakage flow parameters. The measurements were compared against those collected by the mine personnel and found to be within ±5%.

Because the mine utilizes standard concrete stoppings, the study on leakage paths is restricted to a section of the East Mains spanning between crosscuts 29 and 132. The East Mains consist of five entries: two intakes in parallel, two returns in parallel, and one belt line. Figure 4.3 shows the ventilation schematic used to determine the leakage path resistances.

Two factors for Mine B are evaluated: percent ventilation leakage, and leakage path resistance. Based on the quantities of air directed to active workings, old seals, and underground shops, and the quantity of air passed through the main fan, a leakage of 63.6% was determined using Eq. 3.19.

$$L_T = (100) \cdot (393 - 142) / 393 = 63.6\%$$

TABLE 4.2 Leakage path survey data for Mine B*

Item	Measurement/Location	Differential Pressure, Pa	Quantity, m^3/s
1- Primary Ventilation Survey			
	Fan operating point	1790	393.00
	Fan airlock door	1670	na†
	Air-lock doors by overcast	700	na
	Longwall head gate	na	30.90
	Bleeder entries	na	9.50
	Continuous Miner section	na	17.70
	Seals (mine out areas)	na	56.70
	Underground shops	na	9.60
2- Leakage Flow – Intake to Belt			
	Location 1 (intake entry near crosscut 29)	na	152.15
	Path a1, n‡ = 15	168	4.91
	Path b1, n = 1	87	6.05
	Path c1, n = 29	75	7.65
	Path d1, n = 29	60	7.65
	Path e1, n = 29	62	7.61
	Location 2 (intake entry near crosscut 132)		118.51
3- Leakage Flow - Belt to Return			
	Location 4 (return entry near crosscut 29)	na	185.17
	Path a2, n = 15	814	14.17
	Path b2, n = 1	712	1.46
	Path c2, n = 29	553	8.03
	Path d2, n = 29	398	8.03
	Path e2, n = 29	321	7.98
	Location 3 (return entry near crosscut 132)	na	145.49
4- Average Resistance Per Stopping, Ns^2/m^8			
	Intake to belt	757	
	Belt to return	3258	

*Mine B air density = 0.93 kg/m^3.

†na = no measurement.

‡n = number of stoppings per branch.

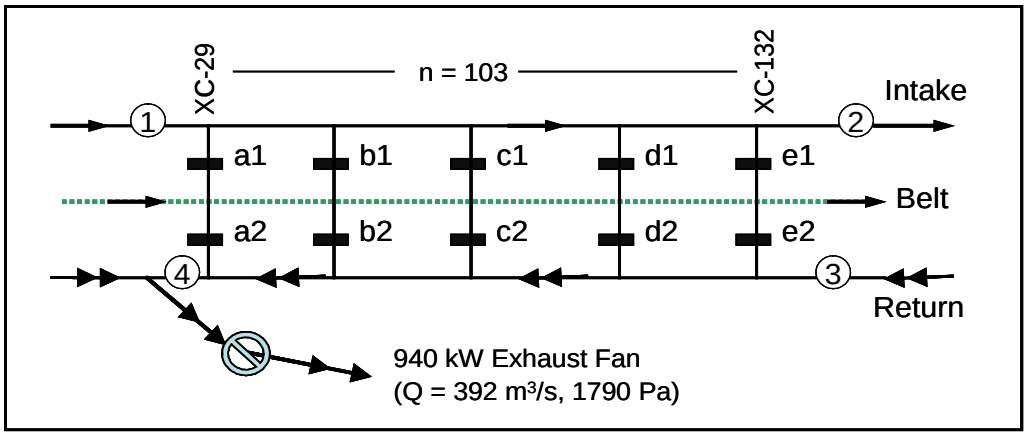

Figure 4.3 Leakage paths in east main entries of Mine B

The leakage path resistances were calculated for two rows of stoppings (intake-line, return-line) located in the East Main section between crosscuts 29 and 132. Table 4.2 shows part of the P-Q measurements taken in this section. Item 2 in the table lists the measurements for the intake-line of stoppings, and Item 3 lists measurements for return-line. Figure 4.4 shows the pressure profiles for the two lines of stoppings.

The graph shows that the pressure difference across stoppings decreases with increasing distance from the surface fan. For similar stoppings, the rate of change follows a decay function with high values near the fan and low values near the workings. Applying equations 3.13 and 3.17 to the Mine B measurements yields the following average individual stopping resistances:

- Intake stopping line: $R_i = 757\ Ns^2/m^8$.
- Return stopping line: $R_i = 3258\ Ns^2/m^8$.

Because of the relative position of the exhaust fan, the return-line stoppings are subject to higher pressure differences than the intake-line stoppings.

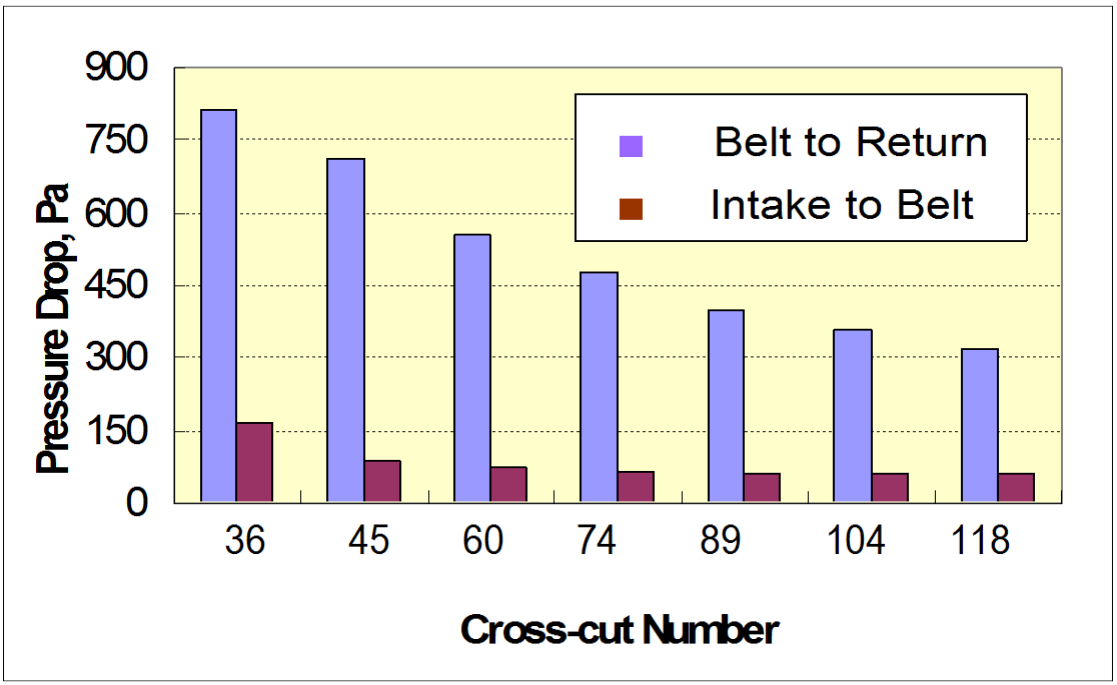

Figure 4.4 Pressure drop across stoppings

4.3 *Summary of Field Survey Results*

A summary of the field survey data is shown in Table 4.3. The results indicate that Omega stoppings have a lower resistance than Kennedy and concrete stoppings. However, this is not necessarily the case. At first glance, the stoppings at Mine A (exclusively Omega block) appeared to be in reasonably good condition. However, with closer visual inspection, it was noted that the stopping sealant that was originally applied had since dried out and no longer had any sealing effect. Mine A personnel reported that stopping inspections were a low priority and that there was no systematic upkeep of the stoppings other than addressing major problems reported in weekly examinations.

In Mine B, the magnitude of the differential pressure across the return line stoppings was much greater than that of the intake line stoppings. The main reason for this is that the belt entry air is also used to supply fresh air to the active workings. This

TABLE 4.3 Summary of field survey results

Parameter	Mine A	Mine B
Mining Method	Room and Pillar	Longwall
Development distance, km	< 1.6	> 19
No. of intake portals	1	7
No. of exhaust portals	1	1
Average entry height, m	2.59	2.90
Average entry width, m	5.94	5.79
Fan pressure, Pa	500	1800
Total fan quantity, m^3/s	60	392
Total percent leakage, %	40	64
Individual stopping resistance, Ns^2/m^8	112 (older Omega) 320 (newer Omega)	757 (Kennedy) 3258 (concrete)

means that the intake and belt airflow paths are in parallel and that fresh air is "intentionally leaked" or fed into the belt entry using regulators. This causes the intake stoppings to have artificially low resistances.

5 RESEARCH METHODS

Two types of models are used to study leakage in underground coal mines: laboratory and numerical. Data collected in the field surveys were used to design a laboratory model so that a similar representation could be made. Measurements made in the laboratory model were used to calibrate a computational fluid dynamics (CFD) model. The CFD model was then expanded to conduct experiments that were not possible in the laboratory model due to physical constraints. Additional numerical modeling was conducted using a commercially available mine ventilation software program called VNETPC.

5.1 *Coal Mine Laboratory Model*

Scientific experimentation in a real world setting can be difficult and very expensive. Also, many of the variables in a real world setting cannot be controlled as is possible in a laboratory setting. For this purpose, a scaled model of an underground coal mine ventilation system has been constructed at the University of Utah's mine ventilation laboratory. The physical model is built to represent a 1:25 scale of a coal mine entry.

5.1.1 Model Similitude

Similitude is a concept used in the testing of engineering models. A model is said to have similitude with the real-world application if the two share geometric similarity, kinematic similarity and dynamic similarity. Geometric similarity means that the model is the same shape as the real-world application and is usually accomplished by simply scaling down in size. Kinematic similarity means that the fluid flow characteristics are

scaled (streamlines are similar). Dynamic similarity means that the ratios of all forces acting on corresponding fluid particles and boundary surfaces in the two systems are constant. Dimensionless parameters are considered to be the same in both real-world and model cases without respect to scale. Therefore, to satisfy the similarity conditions, as many dimensionless parameters as possible are used for comparison.

The greater the departure from the real-world application, the more difficult it is to achieve similitude. It is often impossible to achieve absolute similitude during a model test. In these cases, some aspects of similitude may be neglected, focusing on only the more important parameters. In fluid dynamics, the most common dimensionless parameter used to analyze similitude is the Reynolds Number (Murphy, 1950). As previously stated, the Reynolds Number identifies the flow-state of the fluid (see Section 3.1.2 and Equation 3.8). If the Reynolds Number is satisfied, the geometric and kinematic criteria are also satisfied (Murphy, 1950).

The lab model was constructed using circular ducts, whereas coal mine airways are noncircular. The hydraulic diameter, D_h, is a common term used to calculate the Reynolds Number for noncircular ducts (Murphy, 1950).

$$D_h = 4A / O \tag{5.1}$$

where

D_h = hydraulic diameter (m)

A = cross sectional area (m^2)

O = inside perimeter (m)

From the field surveys at Mines A and B, the average airway dimensions are 5.79 m (19.0 ft) wide and 2.74 m (9.0 ft) high. For this cross-section, the hydraulic diameter is

3.72 m.

The Reynolds Number for the coal mine airways ranges from 1.8110^5 to 1.43 x 10^6, depending on the local velocity measurement. Similarly, the Reynolds Number for the laboratory model ranges from 7.04 x 10^4 to 2.3 x 10^5. The two ranges overlap, indicating a correlation. In both cases, the state of flow is well within the turbulent range ($N_R > 4 \times 10^3$). The model similitude is summarized in Table 5.1.

5.1.2 Model Description

A plan view of the coal mine model is shown in Figure 5.1. This model consists of 14.6 cm diameter ductwork configured in a common U-shaped ventilation system. The intake and return drifts are joined by five crosscuts. The first four (A, B, C, and D) are kept blocked by interchangeable, perforated gate valves that form leakage paths (stoppings). The last is kept open to represent an active mining section or face. The system is powered by a 2.5-kW centrifugal blower fan equipped with a VFD motor. This allows the motor to be set at any speed ranging from 0 to 60 Hz. When the fan motor is operated at 60 Hz (3600 rpm), the fan circulates 0.48 m^3/s of air with 1500 Pa of static pressure.

Table 5.1 Comparison of fluid characteristics between real world conditions and the laboratory model

Parameters	**Coal Mine**	**Physical Model**
Air density (kg/m^3)	0.92	0.99
Airflow velocity (m/s)	1.1	27
Airway diameter (m)	3.6	0.14
Kinematic viscosity (m^2/s)	1.80 x 10^{-5}	1.77 x 10^{-5}
Reynolds Number (dimensionless)	2.18 x 10^5	2.12 x 10^5

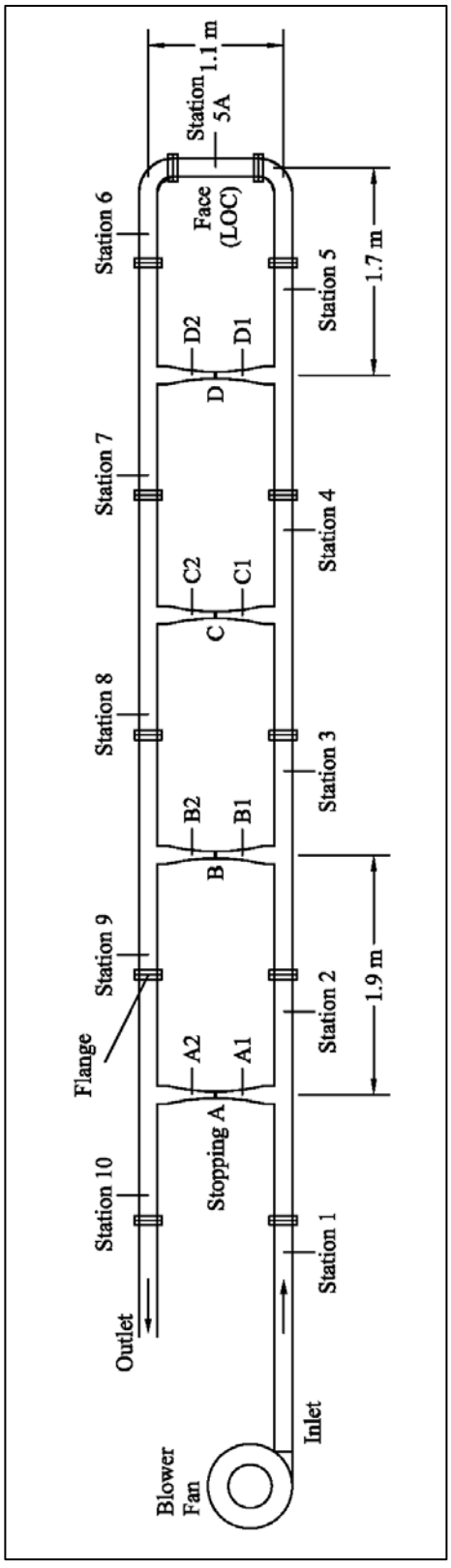

Figure 5.1 Schematic of the University of Utah's coal mine model

There are five sets of perforated, gate-valve "stoppings," having holes of different diameters and numbers as shown in Table 5.2 and Figure 5.2. Any one of the five gate valves can be inserted into any stopping site (A, B, C, or D), allowing a wide variety of stopping configurations. For example, the configuration that allows the smallest amount of leakage in the system is to place gates of type #4 into all four stoppings sites. This ability to vary the simulated stopping resistance makes it possible to represent various types of stoppings having differing resistance values. For instance, gate #4, the closed stopping, can represent a permanent concrete stopping, whereas stopping #0 (fully open) might represent a temporary stopping such as a brattice cloth. The intermediate ones could represent a variety of particular types of stoppings (steel panels, cementitious blocks, concrete blocks). It should be noted that the percent open area is less critical than the gate's hole-configuration. For example, a set of gate valves having a single hole in the center resulting in 27% open area would result in turbulent flow through the gate valve rather than laminar flow, and thus would not result in model similitude.

TABLE 5.2 Perforated gate valves used to represent stoppings

Gate Valve Set	Holes		Open Area, %
	Number	Diameter, cm	
#0 (open)	1	5.6	100
#1	37	0.64	27.2
#2	21	0.64	15.4
#3	21	0.32	3.9
#4 (closed)	0	0	0

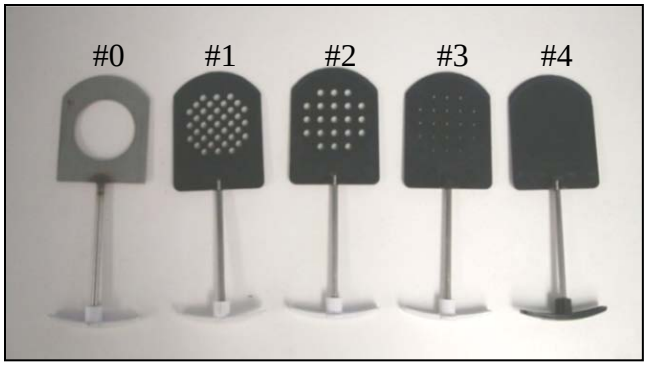

Figure 5.2 Photograph of the gate valves used in the lab

5.1.3 Test Procedure

One complete test consists of measuring static and velocity pressures at each pre-determined station. A test is initiated by inserting a set of gate valves into the stopping slots, setting the fan motor frequency to a predetermined level, and powering the fan. Once the airflow in the system has stabilized, a calibrated manometer and a pitot static tube are used to measure static and velocity pressures. A six-point, equal-area traversing method is used to measure velocity pressure readings from which the average velocity and flow quantity is calculated. This procedure is repeated at each selected station to determine flow quantities throughout the system. Stopping resistances are calculated using Equation 3.13.

5.1.4 Measuring Leakage

Since the duct area in this model is assumed to remain constant (0.0167 m^2), leakage is calculated from the velocity measurements using Equation 3.20. In Figure 5.1, V_T is measured at station 1 and V_F at station 5. The leakage flow through an individual stopping is assumed to be the difference between flows measured on the upstream and downstream sides of the split. For example, the leakage flow through stopping A is the difference between the flows measured at stations 1 and 2, respectively. Assuming that

the quantity of air exiting the system is equal to the amount entering the system, V_T could alternatively be measured at station 10 and V_F at station 6. Similarly, leakage through individual stoppings could be measured using the stations in either the inlet duct or the return duct.

5.1.5 Laboratory Model Results

A complete airflow study was conducted on the lab model using various configurations. Table 5.3 shows an example of the results of a test setup using stoppings of type #1 in positions A, B, C, and D. In this case, the fan motor was set to 30 Hz so that the fan supplied 14.2 m/s of air at 400 Pa of static pressure, resulting in only 8.55 m/s of air reaching the face. The total percent leakage for this configuration was 40%. Directly applying the square law to the measured figures yields resistances ranging from about 181,000 to 482,000 Ns^2/m^8, thus the average for this test configuration is 389,000 Ns^2/m^8. Notice also that the resistance at the face (caused by a wire-mesh screen) was very low in comparison to the stoppings.

A graph of the flow quantities from Table 5.3 is shown in Figure 5.3. The graph shows that over 60% of the total leakage occurs through the first two stoppings, with nearly 40% leaking through the first stopping alone. This trend appears to be an exponential decay function of leakage quantity with distance.

TABLE 5.3 Air P-V measurements across perforated gate valves (size #1 at 30 Hz)

Location	**V, m/s**	**L_T, %**	**Δp, Pa**	**R, Ns^2/m^8**
A	2.24	39.5	255.0	181,084
B	1.30	23.0	207.5	435,403
C	1.09	19.2	160.0	482,167
D	1.03	18.3	137.5	457,291
Face	8.55	na	7.5	365
Fan duty: V_T = 14.2 m^3/min, P_{static} = 400 Pa				

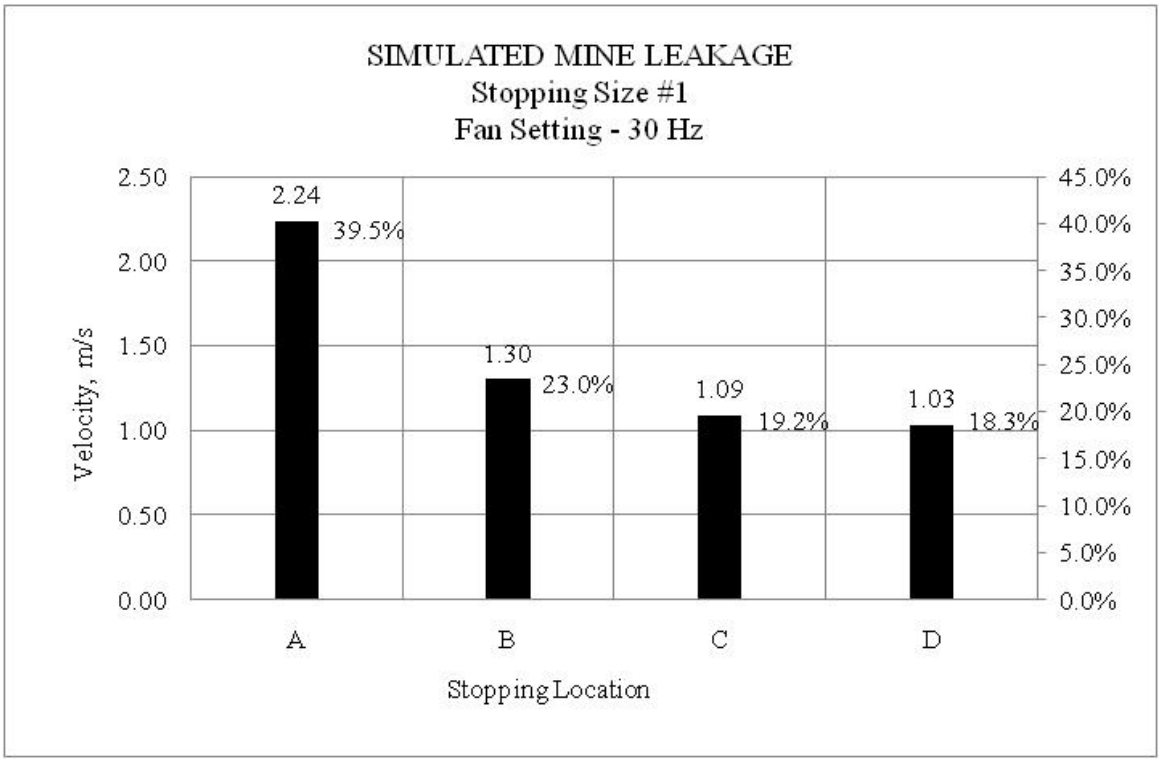

Figure 5.3 Velocity trend of leakage flow through stopping size #1

A summary of the laboratory results for various gate valve settings is given in Table 5.4. The resistance value for each set of gate valves was calculated using all tests in which that type of gate was used. For instance, tests conducted using gates of type #1 included fan settings at 30, 45, and 60 Hz, so resistances calculated from all three tests were used to determine the average value for this set of gate valves. Note in Table 5.4 that the average resistances between each set of gate valves differ by roughly an order of magnitude. In addition, they are orders of magnitude higher than those typically measured in the field. This difference in magnitude is a result of the 1:25 dimensional scale used for the laboratory model. Since R is calculated from Q^2, a scale factor of 625 is applied to the measured resistances. This yields individual stopping resistances that are comparable to field measurements (Koening, 1987; Duckworth et al., 1995; Oswald, 2008).

TABLE 5.4 Laboratory model leakage and resistance characteristics

Gate Valve	Resistance	Resulting Percent Leakage				Scaled Resistance, Ns^2/m^8
	Ns^2/m^8	30 Hz	45 Hz	60 Hz	AVG	
#0 (open)	6.40E+04		62.2	61.8	62.0	102
#1	3.58E+05	39.8	39.9	41.2	40.3	573
#2	1.03E+07	25.6	25.6	24.4	25.2	16,480
#3	3.59E+07		2.9			57,440
#4 (Closed)	5.51E+07		<3			88,160

Based on the scaled resistances, the gate valves can be correlated to real-world control devices:

- Gate #0 = a temporary/poorly constructed/damaged stopping
- Gate #1 = a stopping in poor to good condition
- Gate #2 = a stopping in good to excellent condition
- Gate #3 = a new, ideally constructed stopping
- Gate #4 = a permanent gob seal

5.2 *Computational Fluid Dynamics (CFD) Model*

The primary purpose of the physical lab model was to obtain measurements that could be used to calibrate a computer model so that more extensive and complicated configurations could be examined. In this case, the numerical modeling was done using FLUENT, the CFD module of ANSYS Workbench 12.0 software (ANSYS, 2009a).

The FLUENT software code is based on finite element methods (FEM) and is capable of modelling essentially all aspects of fluid flow: compressible/incompressible, viscous/nonviscous, steady/unsteady, laminar/turbulent, transient, etc. It is user friendly in that it allows users to execute all the commands required to preprocess, solve, and

postprocess the problem. Additionally there are extensive step-by-step tutorials to aid with its extensive applicability. With the program having widespread applicability, extensive training time is required to become a skilled user. Its applicability in mine ventilation is not in modelling the overall mine system, but rather in analyzing detailed fluid flow at specific locations such as the mining face, across equipment, or leakage through stoppings.

Using this software package, a 3-D simulated laboratory model was drawn at 1:1 scale and meshed using the integrated ANSYS Workbench modules ("DesignModeler" and "Meshing"). The Fluent module was used for performing calculations and viewing results. The simulated lab model was calibrated to the laboratory measurements, and then expanded for additional experimentation.

5.2.1 CFD Model Calibration

The CFD model was calibrated to the 30 Hz configuration shown in Table 5.3 above. It was considered calibrated when the critical velocities were within ±5% of the lab measurements as shown in Table 5.5.

TABLE 5.5 Laboratory and CFD model correlation using average velocity (m/s)

	Station				
Model	**1**	**2**	**3**	**4**	**5**
Lab	14.20	11.98	10.68	9.59	8.55
CFD	13.75	11.93	10.58	9.37	8.51
% Difference	3.20	0.40	0.90	2.30	0.50

The input parameters resulting in model calibration are shown in Table 5.6. As measured in the lab, the inlet total pressure was set to 430 Pa with the initial inlet velocity set at 14.2 m/s. In Fluent, the stopping gates were modeled as porous jumps which are defined by face permeability α (m^2), a pressure jump coefficient C_2 (m^{-1}), and the gate thickness Δn (m). The permeability and pressure jump coefficients were derived from the pressure and velocity measurements. This derivation method is shown in Appendix B. The last open crosscut contains a wire-mesh screen that provides some resistance, so it too was modeled as a porous jump, again, providing only slight resistance compared to the gates, as was the case in the physical model.

TABLE 5.6 Input parameters used in Fluent to replicate the lab model (Gate #1, 30 Hz)

Name	Boundary Type		Boundary Condition	Units	Description
Inlet Face	Pressure inlet		430	Pa	total pressure (fixed)
Inlet Face	Velocity inlet		14.2	m/s	initial inlet velocity
Outlet Face	Pressure outlet		0	Pa	total pressure
A,B,C,D	Porous Jump	α =	2.7×10^{-8}	m^2	Permeability
		C_2 =	1000	m^{-1}	pressure jump coefficient
		Δn =	0.003175	m	gate thickness
Open Crosscut	Porous Jump	α =	2.0×10^{6}	m^2	Permeability
		C_2 =	134	m^{-1}	pressure jump coefficient
		Δn =	0.003175	m	screen thickness

5.2.2 Results of the Calibrated Model

Figure 5.4 shows: (a) the CFD model geometry, (b) contours of velocity, and (c) contours of static pressure. In Figure 5.4 (a), the stoppings are labelled as: A, B, C, and D. Several other key locations are also indicated for future reference.

In Figure 5.4 (b), red contours indicate higher velocities and blue contours indicate lower velocities. Leakage in the system is indicated by the rapid change in velocity at each crosscut intersection. The leakage distribution is also shown on Figure 5.4 (b) with 35% passing through the first crosscut, 26% through the second, 21% through the third, and 19% through the last.

In Figure 5.4 (c), the static pressure is highest at the inlet where the fan is located and gradually decreases as the air travels through the duct to the outlet, at which point it is zero. High pressure differentials are indicated by an abrupt change in color as is the case at each of the stoppings. The highest pressure differential is across Stopping A. The pressure drop across the face is gradual as with the inlet and return ducts. Shock loss caused by the 90° turns is clearly identified not only by pressure drop, but also by the disruption in velocity.

Figure 5.5 shows a closer view of velocity vectors near crosscuts A and B. Eddies caused by turbulence can be seen occurring on the inlet side of the crosscut. Also note the velocity variation through the crosscut due to the changes in duct diameter. The air is moving much more rapidly through the stopping gate, which is where the duct diameter is smaller.

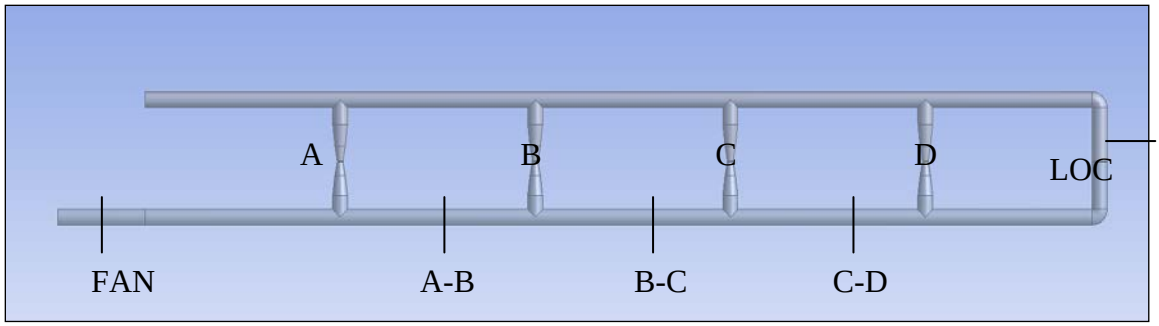

(a) CFD model geometry

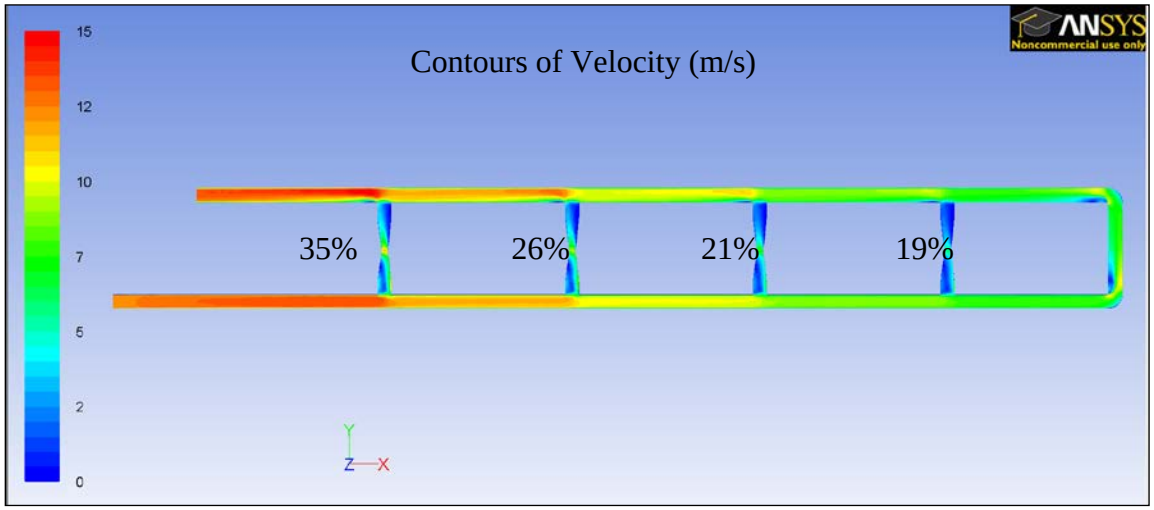

(b) Velocity contours (m/s) of the calibrated CFD model

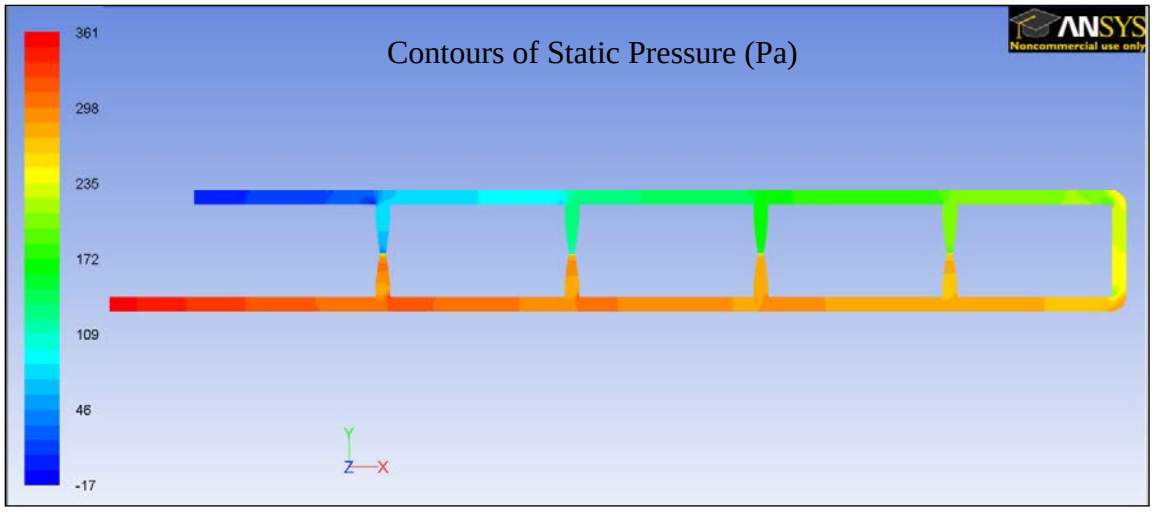

(c) Static pressure contours (Pa) of the calibrated CFD model

Figure 5.4 Fluent output showing CFD model geometry (a), velocity contour lines (b), and static pressure contour lines (c)

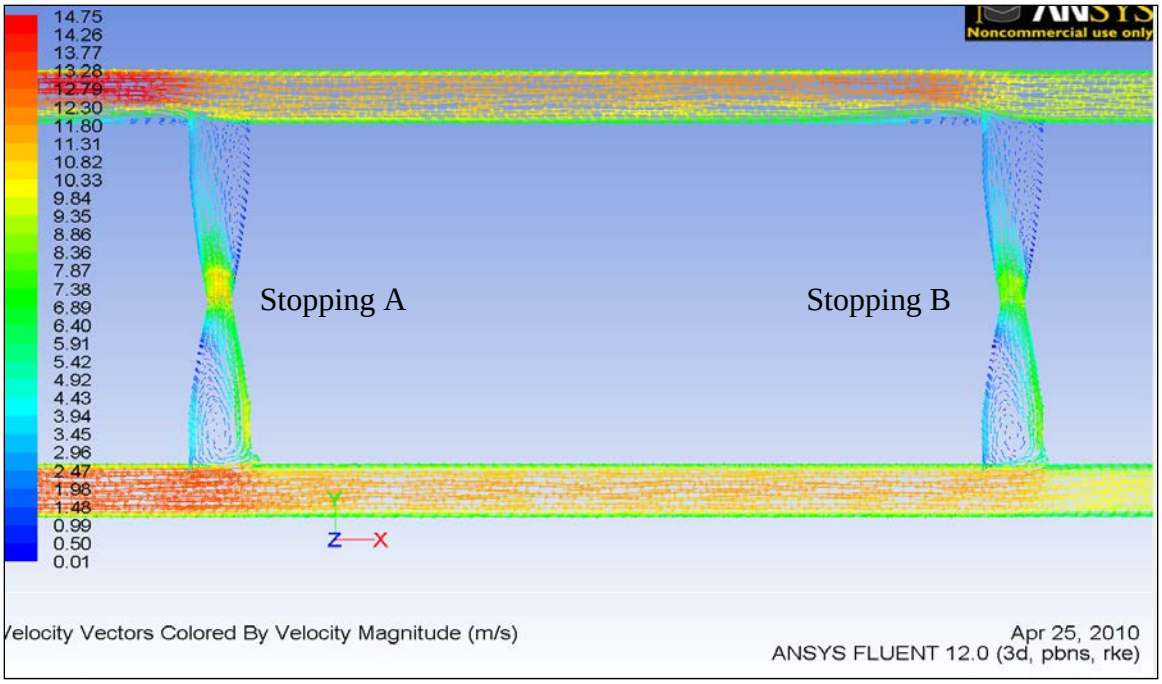

Figure 5.5 Fluent output showing velocity vectors at stopping A (left) and B (right)

Figure 5.6 Shows velocity profiles of vertical sections cut through the intake airway, between crosscuts. The average velocity for each section is indicated in parentheses.

5.3 *Numerical Modeling Using VNETPC*

Computer simulators play a crucial role in mine ventilation. The ultimate advantage in computer modeling is the ability to predict results based on specified conditions and the ability to make changes and obtain the new results.

There are a number of software packages available that are developed specifically for mine ventilation simulation; one such program is VNETPC 2007, developed by Mine Ventilation Services. The program can be used to simulate existing ventilation networks so that fan operating points, airflow rates and frictional pressure drops approximate those of the actual system. This is accomplished by using field survey data. The simulation

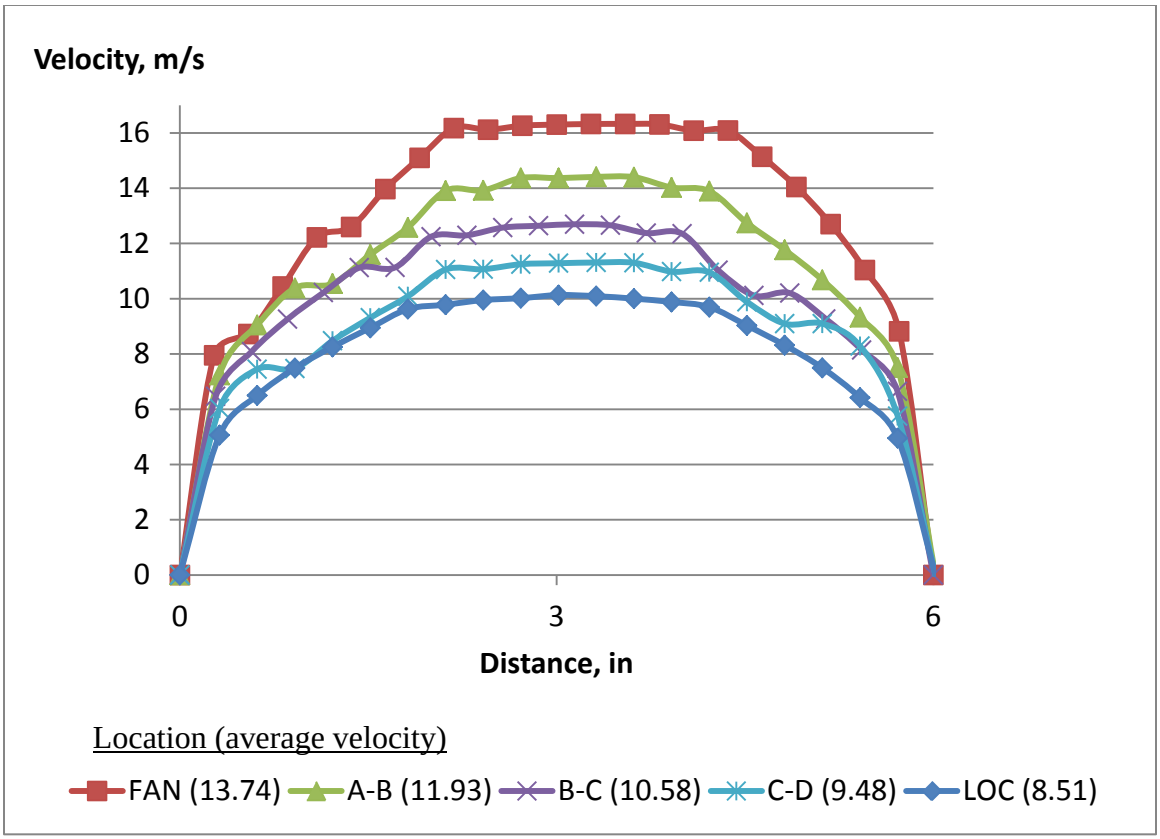

Figure 5.6 Velocity profiles of the calibrated model (average values indicated in parenthesis)

program VNETPC was developed based on the assumption of incompressible flow and on Kirchhoff's first and second laws. The code utilizes an accelerated form of the Hardy Cross iterative technique to converge to a solution (McPherson, 1993).

The VNETPC software is quite user friendly and may be learned relatively quickly. The program is compatible with computer aided drafting (CAD) programs so even complex existing mine drawings can be used to rapidly generate the VNETPC model. Many of the complexities encountered in the real-world can be simplified for the model if needed.

Unlike FLUENT, this program inherently uses all of the common mine ventilation assumptions including that the fluid flow is incompressible, turbulent, and at steady-state.

One major advantage of VNETPC is that computation time for this model was almost instantaneous, whereas with FLUENT, the runtime for a single calculation with this same model typically took on the order of 15 minutes.

5.3.1 VNETPC Model Description (Base Case)

The base case for the VNETPC model is a 2-entry CM development section whose layout closely resembles the laboratory model. A line plot indicating branch numbers is shown in Figure 5.7. The network consists of 17 branches:

- section intake entries (branches 1 through 5),
- section return entries (branches 6 through 10),
- section leakage paths (branches 11 through 14),
- section last open crosscut (branch 15),
- main intake entries (branch 16), and
- main return entries (branch 17)

The dimensions used are an average of those measured in the field surveys. Entries are 5.79 m (19 ft) wide and 2.74 m (9 ft) high with 36.6 m (120 ft), center-to-center pillar lengths between crosscuts. Each leakage path represents 10 stoppings and each airway branch represents a distance of 365.8 m (1,200 ft), thereby making the section development (branch 1 through branch 5) a distance of 1,500 m (4,920-ft). The airway branches were assigned average friction values as measured in coal mine surveys (Prosser and Wallace, 1999). The input parameters for the base case are shown in Table 5.7.

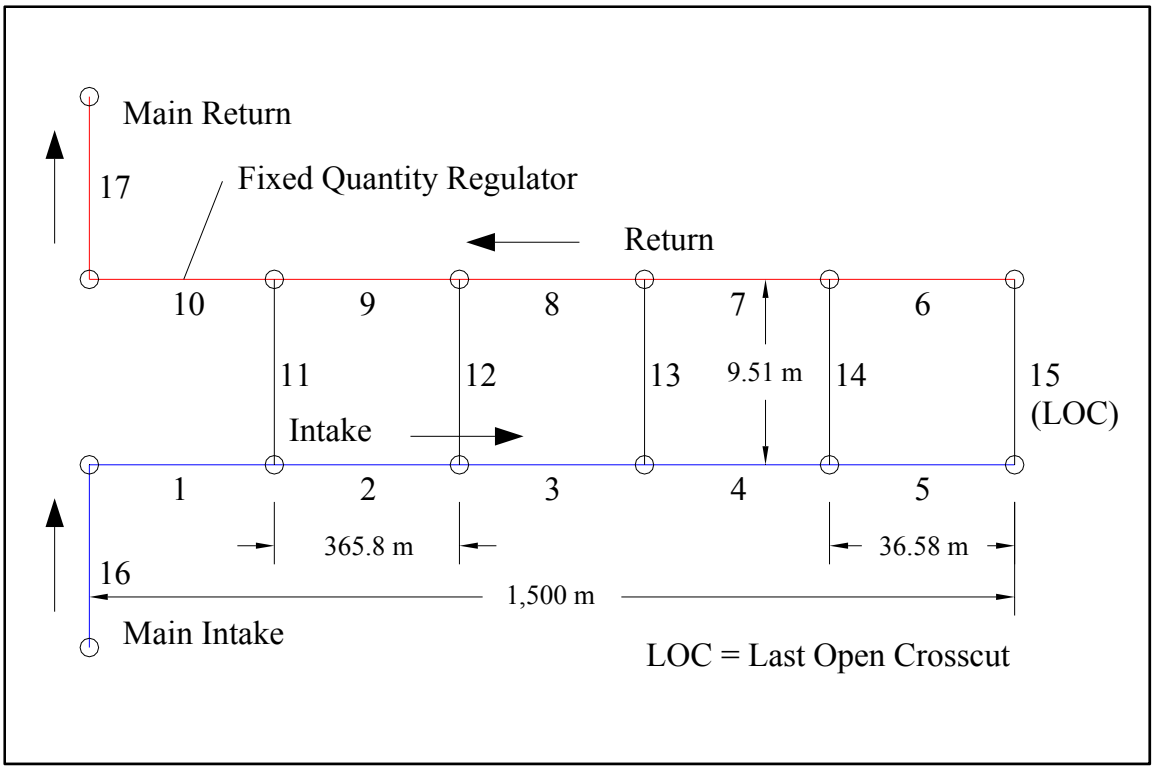

Figure 5.7 A line diagram of a VNETPC network representing 2-entry longwall panel development

TABLE 5.7 Input parameters of the VNETPC model base case for average conditions

Model Parameters	Units	Intake Entries	Last Open Crosscut	Return Entries	Leakage Paths
K-factor	kg/m^3	0.00753	0.00753	0.01058	
Area	m^2	15.9	15.9	15.9	
Perimeter	m	17.1	17.1	17.1	
Length	m	356.8	15.2	365.8	
Resistance	Ns^2/m^8	0.01167	0.00048	0.0165	40
Branch number		1-4	15	7-10	11-14

During 2-entry development, the belt entry is used as the return air course so a k-factor of 0.01058 kg/m^3 is assigned. The k-factor for the last open crosscut is assumed to be the same as the intake entries (0.00753 kg/m^3). The resistance of a single stopping in average condition is assumed to be 4,000 Ns^2/m^8 (Oswald, 2008). Using Equation 3.13, the leakage path branches (N_a = 10) are assigned an R_e value of 40 Ns^2/m^8. An air quantity of 15 m^3/s needed at the last open crosscut (LOC) is assumed. Branch 10, where the section return air joins the main return air, is modeled as a fixed quantity regulator in order to meet this last open crosscut requirement. The main fan has a 112-kW motor and can supply 40 m^3/s at 2,000 Pa.

5.3.2 Base Case Results

The results of the base case model are shown in Table 5.8. To meet the last open crosscut requirement, the section regulator (branch 10) was set to16.9 m^3/s. This resulted in 11% leakage for the section. The leakage distribution trend was similar to that of the laboratory model with nearly 40% of the total occurring through the first leakage path. However, in this case a much larger percentage of the leakage occurs through the stoppings closer to the fan with 31% through the second, 22% through the third, and only 7% through the fourth.

Another observation is that the pressure drop across the stoppings nearer to the fan was significantly higher than across the stoppings further from the fan. This was also the case in the laboratory model. One key observation that is unique to the VNETPC model is the magnitude of the pressure drop across the section regulator. The location of this regulator is significant because it controls the magnitude of the pressure across the section stoppings. With the regulator located as close to the main entries as possible, it

TABLE 5.8 Results for the base case VNETPC model

Branch Number	Description	Q, m^3/s	Leakage, %	Δp, Pa
11	XC's 1-10	0.73	38.8	21.4
12	XC's 11-20	0.59	31.4	14.0
13	XC's 21-30	0.42	22.3	7.2
14	XC's 31-40	0.14	7.4	0.7
15	Last open crosscut	15.01		0.1
10	Total	16.90		2710.0
	Leakage	1.88	11.0	

"shields" the section stoppings and the pressure drop across them is minimized. If for some reason the regulator were located near the last open crosscut, the pressure across each of the section stoppings would increase, which in turn would result in higher leakage quantities.

5.4 *Summary of Research Methods*

In general, the results of the laboratory model and the two numerical models are all similar. Since the CFD model is calibrated to the lab model, there are no major variances expected. However, there is one observation worth mentioning. The general trend of the leakage through stoppings is the same in that the majority of the leakage occurs through the stopping closest to the fan. In all three cases, 35% to 40% of the leakage occurs through the first leakage path. Leakage in the CFD model is a little more evenly distributed than in the lab model example discussed. However, the average leakage distribution of all lab experiments, with all gate sizes and all fan settings, was found to be very similar to that in the CFD results. In the VNETPC model, however, much more leakage occurs through the second path (31.4%) and much less through the fourth (7.4%).

This difference is attributed to the difference in the scaled distance between the fourth leakage path and the last open crosscut. In the lab model, the physical distance between the last leakage path (permanent stopping) and the open crosscut is 1.7 m. The distance between each pair of leakage paths is 1.9 m.

In the VNETPC model, each leakage path represents 10 crosscuts so the distance between each pair of leakage paths is 365.8 m (1,200 ft). However, the distance between the fourth leakage path (last permanent stopping) and the last open crosscut is only 36.58 m (1 crosscut). In practice, MSHA regulation does not allow more than three temporary stoppings between the last open crosscut and the last permanent stopping. If the VNETPC model were drawn to more accurately represent the lab model rather than the real world, the results of the two would likely be very similar. However, it would mean that in the VNETPC model, there would be a distance of 325 m in which no crosscuts were developed, which is not permitted in real-world practice.

This technicality was disregarded in the lab model because in order to obtain accurate velocity measurements in the lab, the flow must have sufficient distance for the velocity profile to fully develop.

The overall percent leakage calculated using Equation 3.19 (see Table 5.4) is approximately the same for a particular total mine resistance (set of gate valves) regardless of the fan setting. This was demonstrated in the laboratory model as well as both numerical models.

6 LEAKAGE CHARACTERIZATION EXERCISES

This chapter describes the leakage characterization exercises that were carried out using numerical modeling. Multiple scenarios were evaluated using both FLUENT and VNETPC. In each scenario, the base case presented in Chapter 5 was modified or expanded in order to observe leakage flow characteristics.

6.1 *Leakage Characterization Using the CFD Model*

The calibrated CFD model was modified from having only four crosscuts to having 10 as shown in Figure 6.1. This layout closely resembles development of a 2-entry longwall gateroad. Two scenarios were evaluated: (1) a single fan system, and (2) the addition of a booster fan at location ST-6. In both cases, it was assumed that a minimum velocity of 8.5 m/s was required at the last open crosscut (Face). The input parameters for both cases are shown in Table 6.1. For this analysis, the pressure jump coefficient of 17,000 m^{-1} is used for the gate valves.

In general, adding a booster fan to any ventilation system should significantly decrease the main fan pressure requirement, which in turn will reduce the overall leakage. The combined operating pressure points of the main and booster fan will typically be similar to, if not less than, the single fan condition. The main advantage of utilizing a booster is this significant reduction in pressure across the stoppings located between the main fan and the booster fan. This pressure reduction effectively lowers leakage quantities through those same stoppings.

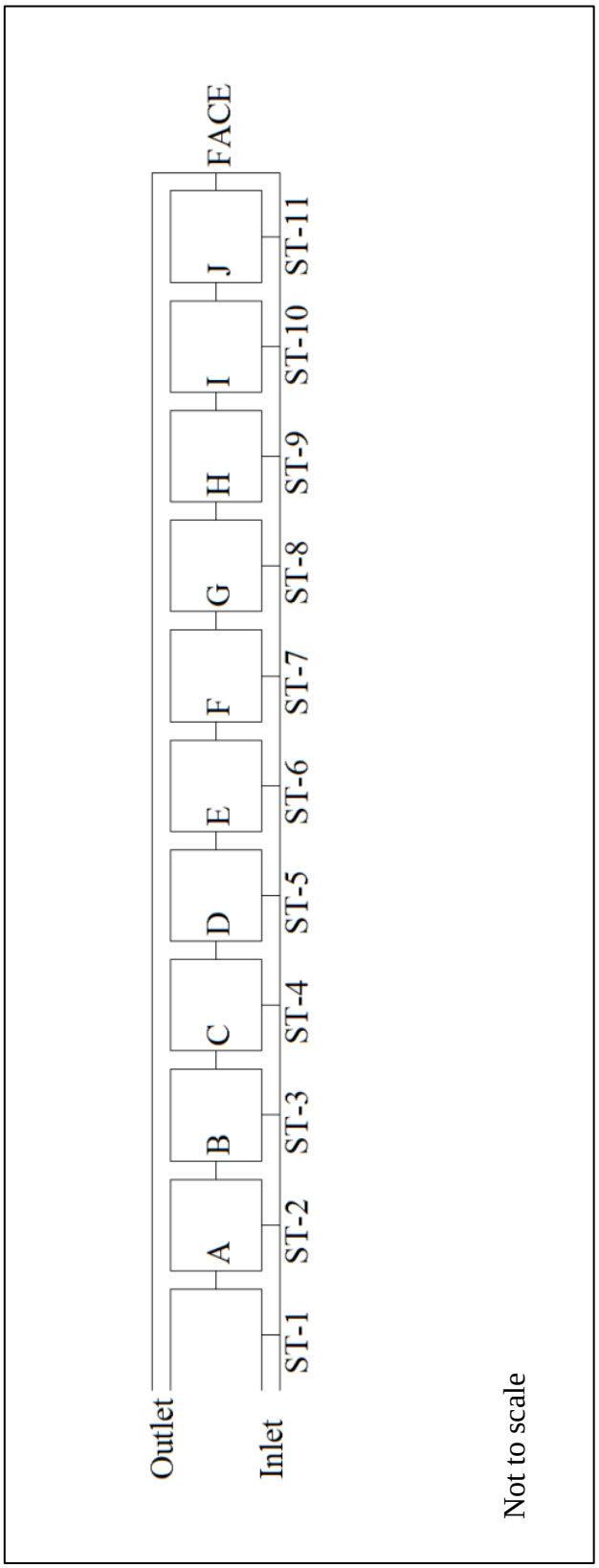

Figure 6.1 Schematic of modified CFD model having 10 stoppings plus an open face

TABLE 6.1Input parameters for case comparison

Name	Boundary Type		Boundary Condition	Description
Single Main Fan				
Inlet Face	Pressure inlet		430	total pressure, Pa
Outlet Face	Pressure outlet		0	total pressure, Pa
Main Fan and Booster Fan				
Inlet Face	Velocity inlet		275	total pressure, Pa
Outlet Face	Pressure outlet		150	total pressure, Pa
Parameters Constant in Both Cases				
		α =	2.7×10^{-8}	Permeability, m^2
A,B,C,D	Porous jump	C_2 =	17,000	pressure jump coefficient, m^{-1}
		Δn =	0.003175	gate thickness, m
		α =	2.0×10^{6}	Permeability, m^2
Open Crosscut	Porous jump	C_2 =	134	pressure jump coefficient, m^{-1}
		Δn =	0.003175	gate thickness, m

The results are shown in Table 6.2. By utilizing the booster fan, the main fan operating pressure was reduced from 430 Pa to 275 Pa. The combined pressure of the two fans was 425 Pa, slightly less than with a single fan. The velocity at the main inlet was also reduced which yielded a 5% overall reduction in leakage.

Comparisons of the pressure, quantity, and leakage trends for both cases are made. Figure 6.2 shows the trend of pressure drop across stoppings. In the single fan case, both exponential and linear decay functions show a good fit, although the exponential function fits slightly better. The aforementioned pressure reduction by the booster fan is clearly indicated.

TABLE 6.2 Summary of results

Parameter		Single Fan	Booster Fan	
			Main	Booster
Input	V_T, m/s	14.4	13.4	
	P_T, Pa	430	275	150
Output	V_F, m/s	8.51		8.57
	L_T, %	41		36

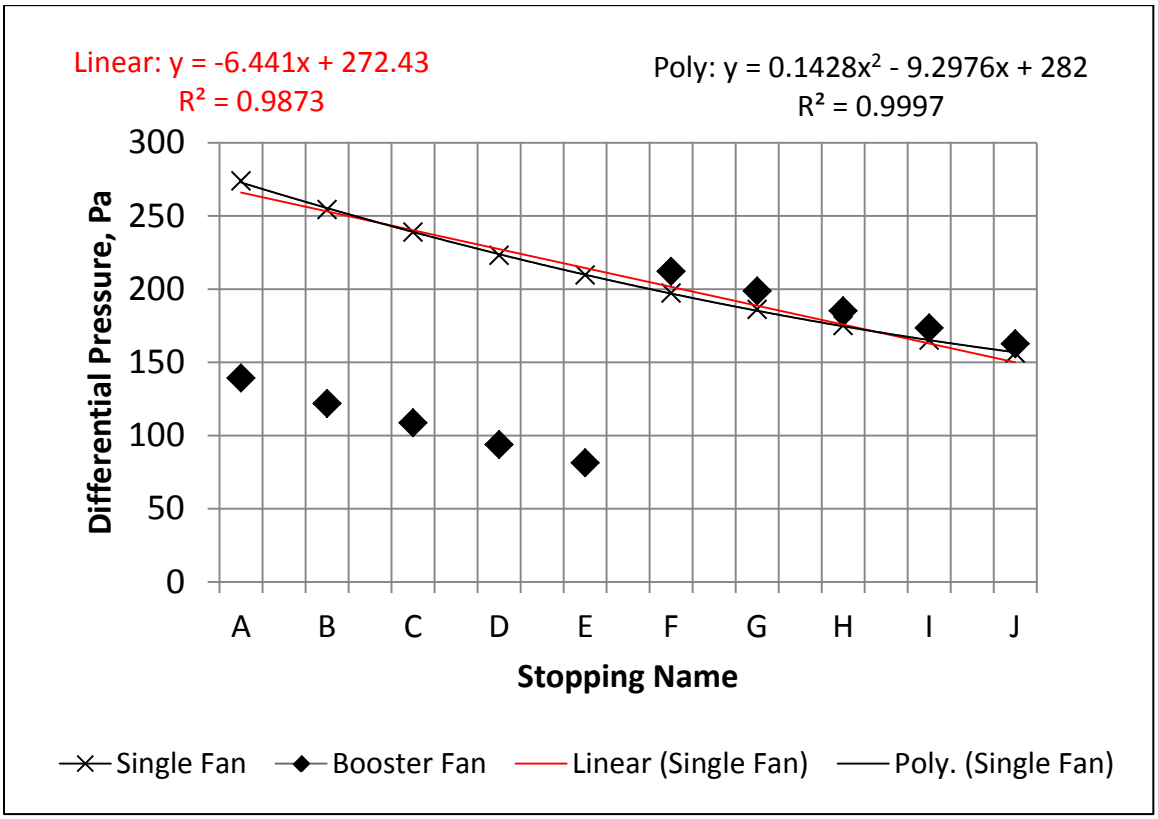

Figure 6.2 Pressure drop across individual stoppings

The pressure drop across the stoppings located between the inlet and the booster fans is dramatically decreased, whereas the pressure drop between the booster fan and the last open crosscut is only slightly higher than in the case with only the single fan. Figure 6.3 shows leakage velocity through each of the stoppings, which is proportional to leakage. The total reduction in leakage is attributed to the pressure reduction between the inlet and the booster fan. The leakage through stoppings A to E is decreased while

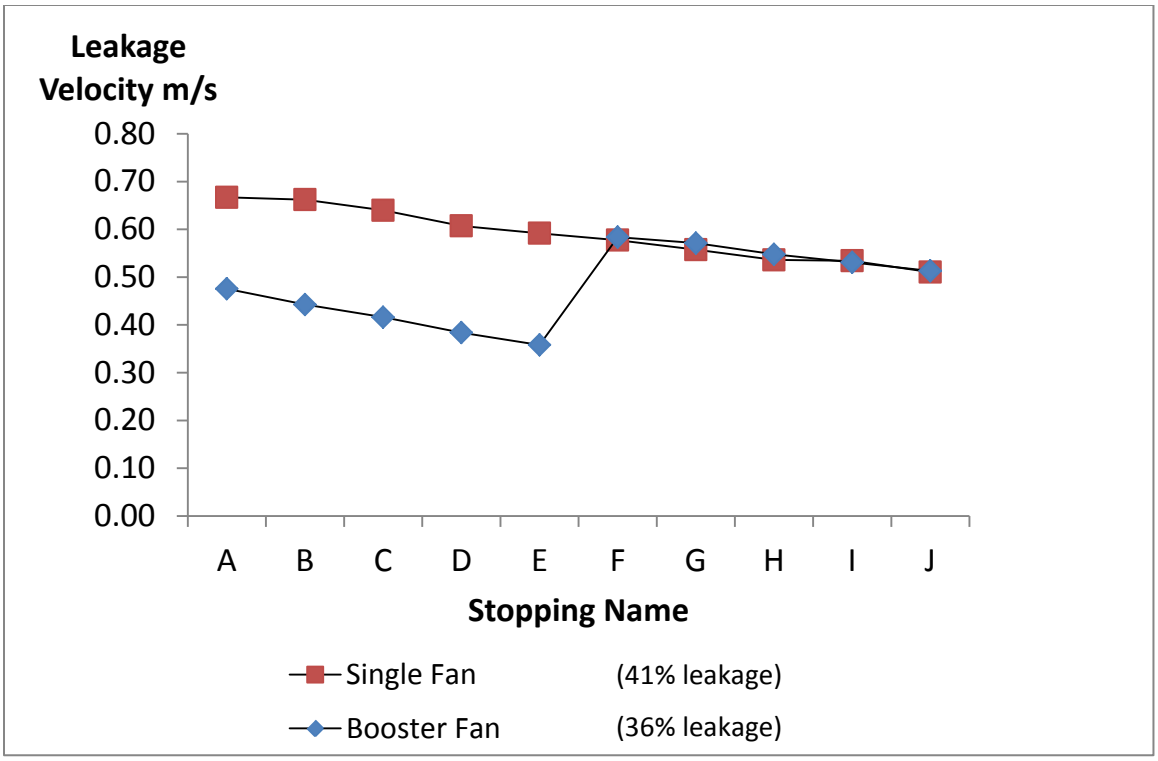

Figure 6.3 Trends of leakage through individual stoppings

through F to J it remains approximately the same. Figure 6.4 shows how the leakage is reduced and redistributed throughout the system. In the single fan case, more than 10% of the total leakage occurs through each of the first five stoppings (A, B, C, D, and E). The addition of the booster fan redistributes the leakage so that the majority occurs through the last five stoppings (F, G, H, I, and J). The space between the general trends of the two scenarios is indicative (although not quantitatively) of the percent leakage reduction. Further spread indicates greater reduction.

The results of this experiment were as expected with the exception of the percent leakage reduction. A greater reduction in leakage was expected in the system with the booster fan. This may be an effect of using constant pressure to simulate the fan. In reality, the fan P-Q operating point in fact is not constant. If a fan curve were used, the results should be more accurate.

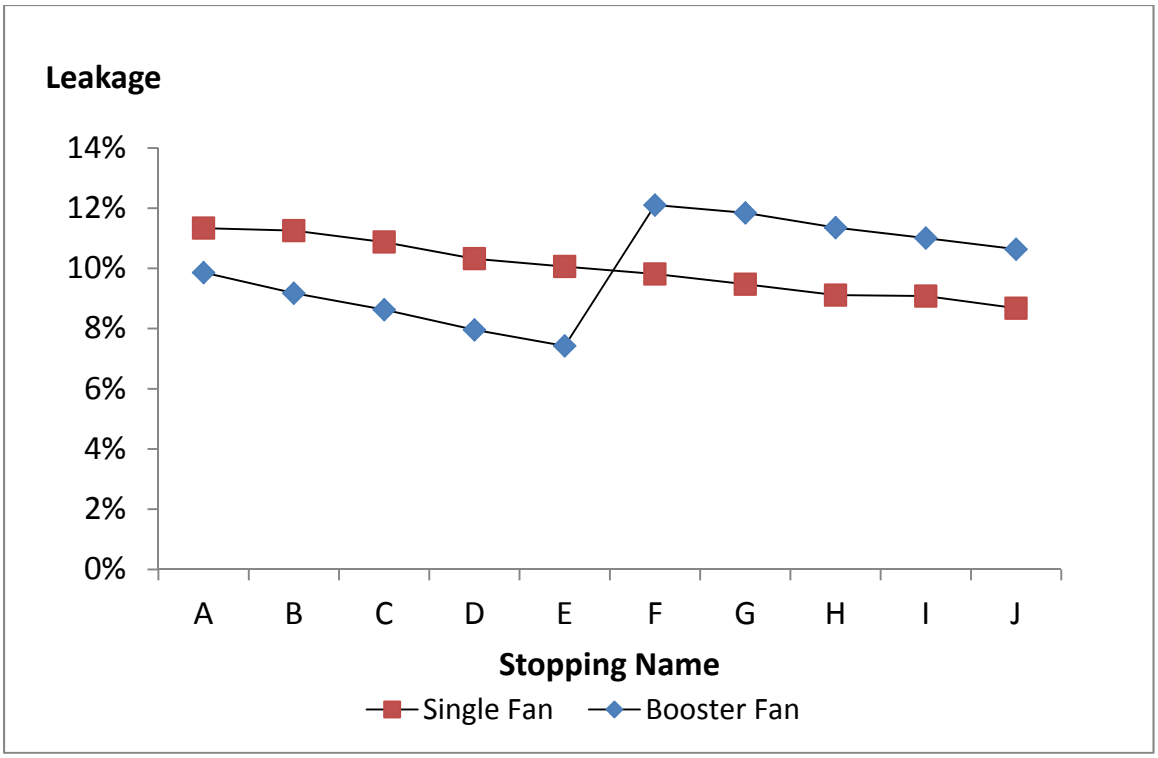

Figure 6.4 A comparison of leakage distribution between a single fan system and a booster fan system

6.2 *Leakage Characterization Using VNETPC*

Numerical modeling using CFD has gained popularity in recent years and its application is becoming more and more widespread. However, the calculations and data reduction can be very time consuming, depending on the size of the simulated model. A number of computational software packages that are less memory intensive, and are designed specifically for mine ventilation simulation are readily available. Some of these programs include VNETPC, MINEVENT, VUMA, MIVENA and Ventsim (Gibbs, 2002). The VNETPC software was used to conduct a wider variety of leakage flow scenarios and comparisons of leakage reduction methods was made. The results are given in this section.

6.2.1 Exercise 1 - Development Stages

The purpose of this exercise was to investigate the changes in leakage that occur gradually as a development section is advanced. This was done using the base model parameters. Since the only change between stages was the number of leakage paths, the only input parameter that was changed was the fixed quantity regulator, which was changed by trial and error until the last open crosscut requirement of 15 m^3/s was met. The individual stopping resistance at all stages was 4,000 Ns^2/m^8 as in the base model case.

The resulting percent leakage for each stage was as follows:

Stage 1: 10 stoppings = 2.0 % (Q_T = 15.3 m^3/s)

Stage 2: 40 stoppings = 10.4% (Q_T = 16.8 m^3/s)

Stage 3: 70 stoppings = 23.5% (Q_T = 19.7 m^3/s)

Stage 4: 100 stoppings = 36.4% (Q_T = 23.6 m^3/s)

6.2.2 Exercise 2 - Stopping Condition

Most leakage is a result of poor workmanship and lack of maintenance (Tien, 1996). The purpose of this exercise was to investigate the difference in leakage between various stopping conditions. In this exercise, the configuration used was Stage 4 from Exercise 1 (100 stoppings). The only parameters that changed were the resistances for the leakage paths (for all stoppings) and the fixed-quantity regulator. They were changed as needed to meet the last open crosscut requirement. The resistances used in this exercise ranged from R_i = 320 to 8,700 Ns^2/m^8. Six different conditions were compared. The values in conditions 1 and 2 are those measured in the field surveys at Mines A and B.

The other four conditions correspond to average stopping conditions ranging from poor to excellent (Oswald, 2008). They are as follows:

Condition 1:	Mine A measurement	(R_i = 320 Ns^2/m^8)
Condition 2:	Mine B measurement	(R_i = 757 Ns^2/m^8)
Condition 3:	Poor	(R_i = 2,000 Ns^2/m^8)
Condition 4:	Average	(R_i = 4,000 Ns^2/m^8)
Condition 5:	Good	(R_i = 6,500 Ns^2/m^8)
Condition 6:	Excellent	(R_i = 8,700 Ns^2/m^8)

In conditions 3 through 6, the regulator was needed which means that the fan was able to supply enough air to the last open crosscut. Using condition 2, the regulator had to be removed in order to allow enough air to reach the last open crosscut. This means that with this fan setting, if the stoppings had any resistance less than 757 Ns^2/m^8, there would not be a sufficient quantity of air reaching the last open crosscut. This was the case using condition 1 in which only 10.4 m^3/s reached the last open crosscut.

Figure 6.5 shows the percent leakage versus individual stopping resistance. Using the resistance measurements from Mine A, the resulting total leakage is 72.3%. When the resistance of these stoppings was improved to average condition (R_i = 4,000 Ns^2/m^8), the total leakage was reduced from 72.3% to 36.4%, nearly 36% improvement in total leakage. Conversely, when the stoppings were improved from average condition to excellent condition (R_i = 8,700 Ns^2/m^8), the total leakage decreased from 36.4% to 27.2%, only about a 9% improvement in leakage. The relationship is a logarithmic trend. This exercise indicates that in practice, more emphasis should be placed on improving

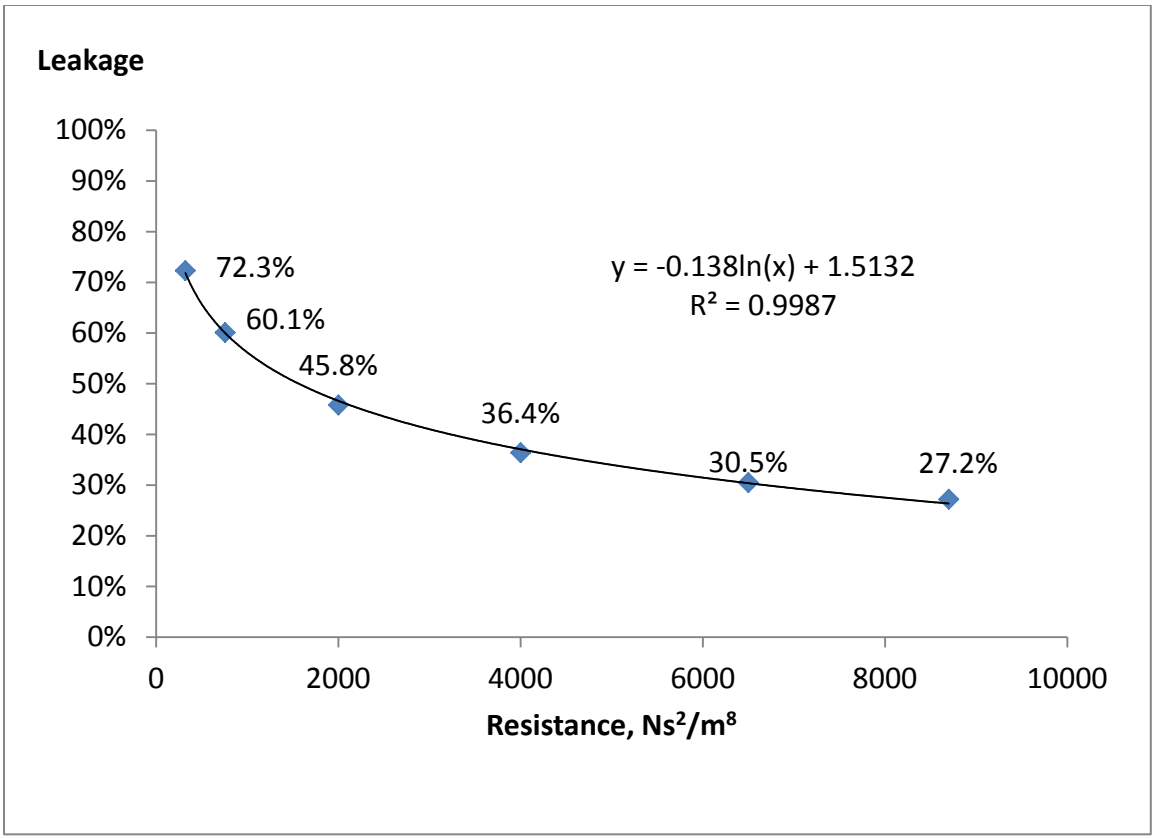

Figure 6.5 Exercise 2 results showing stopping leakage versus individual stopping resistances

stoppings that are in worse condition than those that are in better condition, regardless of where in the mine they are located.

Figure 6.6 shows the leakage profiles of conditions similar to those listed above, along with the two theoretical extreme conditions: 100% and 0% leakage. In the 100% leakage case, the resistance values were assigned such that the branches representing stoppings were modeled as open crosscuts with no stoppings installed. Under these circumstances over 94% of the total amount of air entering the mine was short-circuited directly to the return entries through the first 10 stoppings.

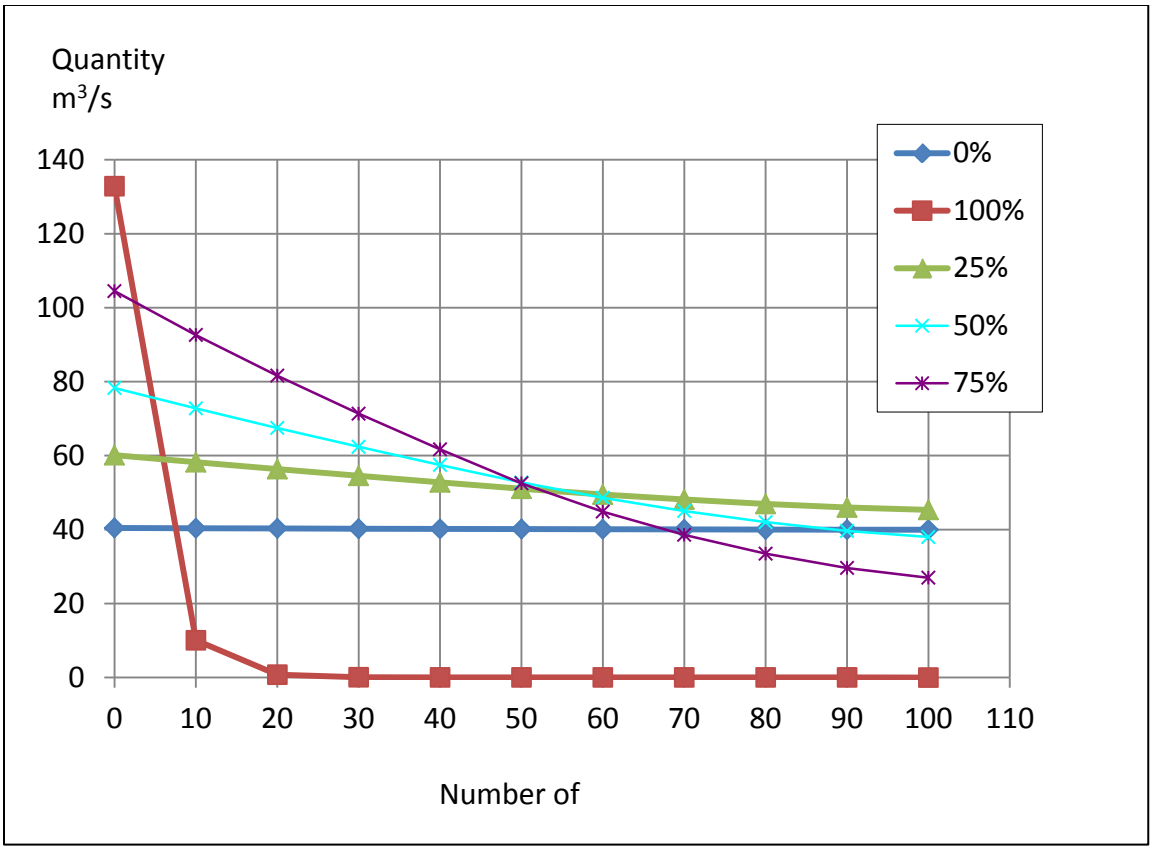

Figure 6.6 A comparison of leakage profiles

In the near 0% leakage case, all of the stoppings were assigned the maximum resistance value allowed by the VNETPC program (100,000 Ns^2/m^8). Under these circumstances, there was essentially no leakage in the system and virtually all of the air entering the mine reached the working face. This resembles a case where there are no connecting crosscuts between intake and return entries. The three realistic conditions show that when the leakage is higher, the profile resembles more of a decay function, whereas the lower leakage curves exhibit a linear trend.

This exercise emphasizes the importance of having good workmanship on the initial installation of a permanent stopping, and a regular stopping maintenance program to keep the stoppings in reasonably good condition.

6.2.3 Exercise 3 - Recommended Stopping Maintenance Program

In the real world, when stoppings are initially installed, they typically have a relatively high resistance. Over time, the stoppings are exposed to wear and tear from a variety of sources, which decreases their resistance. Assuming all of the stoppings are constructed in the same manner and using the same materials, older stoppings will have lower resistance than newer stoppings. It was previously demonstrated in this study that the stoppings near the fan allow greater leakage than those near the section heading due to higher pressure differentials. When this is combined with age-based deterioration, even more leakage will occur through the stoppings near the fan as mining progresses. By this reasoning, leakage reduction methods should be focused on the stoppings near the fan. A series of experiments was conducted in order to determine a "critical area" in which the stopping maintenance program should be focused. This was accomplished by again using the configuration of Stage 4 of Exercise 1 (100 stoppings), in conjunction with using Conditions 3 through 6 of Exercise 2.

For this exercise, it was assumed that all stoppings are initially in poor condition (R_i = 2,000 Ns^2/m^8). The leakage distribution in this initial condition is shown in Table 6.3. In this case the critical leakage location was the first 10 stoppings since this was where the majority of leakage (17.4%) occurred. When only the first 10 stoppings were improved to average condition (R_i = 4,000 Ns^2/m^8), the total percent leakage was only slightly reduced from 45.8% to 44.5%. The leakage that occurred through the first 10 stoppings was reduced from 17.4% to 13.0%, and the new critical location became the next set of 10 stoppings through which the majority of leakage occurred, in this case, stoppings 11 through 20.

TABLE 6.3 Leakage distributions for 100 stoppings in poor condition (46% leakage)

Stoppings	Leakage
10	17.4%
20	15.8%
30	14.1%
40	12.5%
50	11.0%
60	9.6%
70	8.0%
80	6.5%
90	4.5%
100	0.5%

This pattern of improvement was continued. After the first 40 stoppings were improved, the first 10 stoppings again became the critical leakage area through which the majority of leakage occurred, although the leakage was now more evenly distributed. At this point, the first 10 stoppings were improved to good condition, having R_i = 6,500 Ns^2/m^8.

This iterative improvement process was continued until the first 10 stoppings were in excellent condition, where R_i = 8,700 Ns^2/m^8, and were again the critical leakage area. At this point in the iteration process, the stopping conditions and associated leakage distribution were as shown in Table 6.4. The leakage has been reduced from 45.8% (prior to any improvements being made) to 33.3%; a significant reduction in overall leakage.

The condition column in Table 6.4 can be used as the basis for creating a systematic stopping maintenance program, indicating the priority of stopping maintenance in each area of the section. For comparison, if no prioritizations were used

TABLE 6.4 Leakage distribution for 100 stoppings after stopping maintenance (33% leakage)

Stoppings	Leakage	Condition	Priority*
10	13.1%	Excellent	H
20	12.0%	Excellent	H
30	12.7%	Good	H/M
40	11.5%	Good	H/M
50	10.3%	Good	M
60	11.5%	Average	M/L
70	9.6%	Average	M/L
80	10.9%	Poor	L
90	7.6%	Poor	L
100	0.8%	Poor	L

*H = high, M = medium, L = low.

so that all 100 stoppings were improved and maintained in excellent condition, the resulting total leakage is 27.2%; only a slight advantage over the 33.3% resulting total leakage as shown in this case.

6.2.4 Exercise 4 - Fewer Crosscuts (Longer Pillars)

In this exercise, overall leakage was reduced by using pillar lengths that were twice that of the base case. Beginning again with 100 stoppings in poor condition, this scenario was modeled in VNETPC by changing the stopping resistance values to represent only 50 stoppings in the same total development distance. The resulting total leakage was just 28.2%. This is comparable to maintaining 100 stoppings in excellent condition (27.2%) and is the most effective leakage reduction method of those considered. When the prioritization method previously described in Exercise 3 was used, the total leakage was further reduced to only 19.2%.

6.3 *Summary of VNETPC Modeling Results*

The leakage studies conducted using VNETPC show that:

(1) Leakage continually increases during normal mine development by the necessary addition of leakage paths.

(2) The condition of the stoppings plays a very important role in the leakage trend. If stoppings are constructed and maintained poorly, the leakage distribution trend is more similar to that of the square law, and the nature of flow tends toward being turbulent. If stoppings are well constructed and maintained, the leakage distribution trend is more linear in nature and the flow tends to be laminar.

(3) Prioritizing leakage upkeep with a systematic stopping maintenance program which focuses on stoppings near the fan reduces leakage nearly as much as maintaining all stoppings in the same excellent condition.

(4) Minimizing the number of leakage paths is the most effective method of reducing leakage.

7 DISCUSSION AND CONCLUSIONS

7.1 *Field Surveys*

In general, the resistances calculated from the field survey measurements are considerably lower than those reported in the literature although there was no systematic method used to measure the condition of the stoppings.

As was the case with Mine A, Mine B personnel stated that the company had no systematic method of maintaining stopping conditions, although during the visit to the mine, one foreman reported to the ventilation engineer that some repairs were needed for a number of ventilation structures. At Mine B it appeared that many of the intake line stoppings were intentionally not kept air tight. The average pressure drop across 87 of the 103 intake-line stoppings at the mine was 65 Pa, presumably related to the use of “belt air.”

The return-line stoppings were obviously quite old as evidence of the extensive buildup of rock dust on the floor in the return entries. As with the stoppings at Mine A, the majority of stoppings appeared to be in good condition from initial visual inspection. However, in contrast to those at Mine A, with the Mine B stoppings, there was no apparent or obvious method that could be used to improve their condition beyond what it was. It was obvious, however, that the material used in constructing the return line stoppings was intended for long term use.

For comparison, Mine A had 40% overall leakage in 1.6 km of development whereas Mine B had 64% overall leakage in 19 km of development. At first glance, Mine

A may appear to be better than Mine B in terms of overall leakage. However, in light of the considerable difference in development distance between the two, this is not the case. A correlation can be made to one of the VNETPC leakage exercises (Exercise 1 - Development Stages). In this exercise, an increase in development distance by a factor of 10 (from 10 stoppings to 100 stoppings) increases the percent leakage by 34%. This is with stoppings in average condition. The development distance of Mine B is about 12 times greater than Mine A. Therefore, conceptually if Mine A were as extensive as Mine B, it would likely have greater than 75% leakage. Furthermore, since the stoppings at Mine A have lower resistances than those at Mine B, the percent leakage would be even higher. The general condition of the stoppings at Mine A greatly limits its long term expansion possibilities.

Regarding Mine B, the fan is centrally located with respect to the workings to allow a flow-through ventilation method wherever possible. This makes the percent leakage much lower than it otherwise would be. In the areas where the flow-through system is used, there is essentially no leakage because the intake airways simply become return airways after the air passes the working areas as opposed to the air traveling in opposite direction through parallel separated entries as with the U-type ventilation method.

7.2 *Laboratory Model*

The lab model was limited to only five crosscuts due to the physical constraints of the space available as well as the size of the fan. In practice, a recommended rule of thumb is to make velocity measurements at a minimum distance of four times the diameter of the opening on the upwind side of a split and a minimum distance of 10 times

the diameter on the downwind side. Due to the limited amount of space available in the lab, it was not possible to do this. The limited space availability is also the reason why the crosscuts were reduced in diameter for the gate valves.

The variety of gate valve configurations available for use in the laboratory model makes it possible to simulate the flow conditions at both mines. The state of flow through all of the stoppings that were measured at Mine A was always turbulent. This is in contrast to publications which suggest that flow through stoppings may be assumed to be laminar (Ralph, 1983). This is further indicative of the poor condition of the stoppings. In the lab model experiment using gate valve #1 (27% open area) in all locations resulted in turbulent flow through all of the leakage paths. Using gate valve #3, all of the leakage flow was either in the laminar or transitional region, which was more similar to the conditions at Mine B. In the experiments with gate valve #2, flow was turbulent through stoppings A, B, and C, but laminar through stopping D.

7.3 *CFD Model*

Although the lab model was accurately replicated in the CFD model, there are some notable differences. Firstly, the physical model contains joints located throughout the ductwork that would seemingly cause some additional turbulence. There was no attempt to replicate this because the joints were connected in such a way as to minimize this effect.

Secondly, the CFD model showed good velocity profiles throughout the inlet side of the ductwork, but velocity profiles on the outlet side of the ductwork fluctuated significantly. This conforms to what is expected in that the splitting of an airway should

cause less turbulence than joining airways. In the lab model, measurements in the outlet ductwork seemed to give more consistent velocity profiles than those in the inlet stations.

The CFD modeling in this study was limited to characterizing leakage flow at the laboratory model scale. This was in part due to the time that is required to conduct a wide variety of experiments, particularly in 3-D.

One of the difficulties that would be encountered in using Fluent for a real-world scale model is that of accurately accounting for wall roughness. The Fluent User's Guide (2009) gives some guidance into assigning accurate wall roughness coefficients for smooth-surfaced as well as for tightly-packed, uniform sand-grain roughness, but further states that a clear guidance for choosing the proper roughness constant for arbitrary types of roughness is not available. Nevertheless, a reasonable effort could be made.

Fluent also has the capability for input of fan curve data rather than simply applying constant pressure at the inlet face as done in this study. This would yield more accurate results.

7.3.1 Porous Jump Parameters

A sensitivity analysis was conducted on the parameters used to define a porous jump (C_2 and α). The pressure jump coefficient (C_2) had the most profound effect. When C_2 is large (> 10,000 m^{-1}), the effect of α is overshadowed. For the CFD model, the combined effect of these values is equivalent to the resistance of the stopping. Alternatively, either one could be used without the other in the calculation. Since C_2 has the most profound effect, its correlation with percent leakage was determined. The relationship is shown in Figure 7.1. Note that the trend is very similar to that of individual stopping resistance modeled in VNETPC.

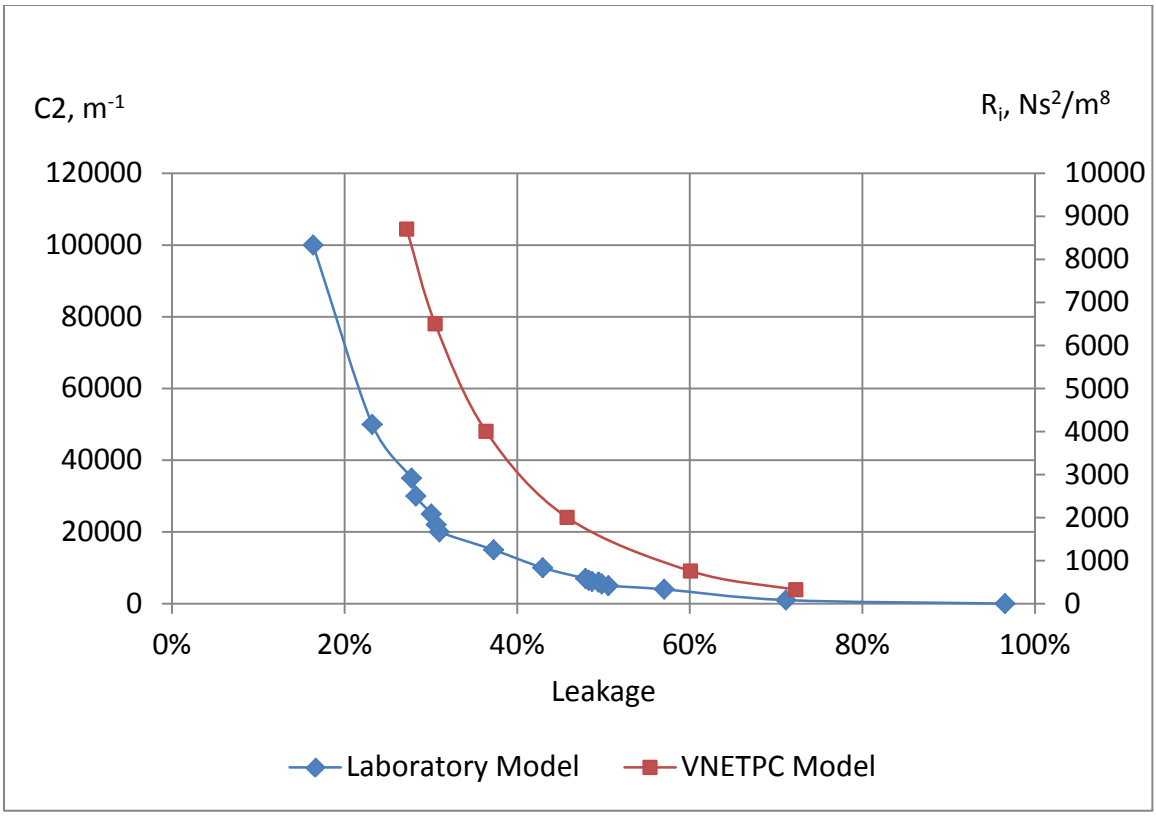

Figure 7.1 Correlation between the laboratory gate valve model, C_2 and and real-world individual stopping resistance, R_i

7.4 *VNETPC Model*

Although the studies were conducted for application to a two-entry longwall gateroad development section, the results can be applied to an entire mine. In addition, the approach in Exercise 2 is from the perspective of a mine that is already active. However, the recommended program is perhaps more advantageous for a green-field project. The number of stoppings ranging from 0 to 100 should be thought of in terms of percent development of the maximum development distance for a given project. The higher priorities assigned to the stoppings near the fan are not only indicative of the areas where stoppings should be maintained, but also where long-term decisions are more critical. For example, it is more valuable to maximize pillar lengths in the first 20% of the

mine workings than anywhere else. Likewise, stoppings in this area should be built with stronger materials than in the more distant areas. For example, gob seal designs that are no longer adequate under the new seal regulations could instead be used as stoppings in the high-priority areas. The designs could be modified as needed to accommodate personnel doors and other needs as required.

Another method of reducing leakage not considered in the VNETPC exercises is that of developing parallel entries near the main fan. The main reason that this method was not analysed is that it is already commonly practiced. In terms of mine planning, the same approach as suggested for choosing pillar lengths should be used.

7.5 *Recommendations*

Based on the results of this study, further research should be conducted. The CFD model which has been calibrated to the physical model should be scaled to real-world conditions. A one to one scale model of 100 real world crosscuts should be developed for direct comparison with the 100 crosscut exercises conducted using VNETPC. The model could be drawn in such a way as to simulate leakage through both the permanent and temporary stoppings in the section. In a real-world scaled model, leakage through individual stoppings or seals could be modeled.

Having developed Table 6.4 which prioritizes the specific locations where stopping maintenance is needed, detailed stopping maintenance programs could be developed for each common type of stopping based on its relative location within the mine. The maintenance program should include among other components, the frequency of maintenance activities such as periodic checks and repairs that are needed in each area

of the mine. The recommended maintenance activities should be correlated with the pressure profile.

Finally, only preliminary experiments were conducted in which a booster fan was used to reduce leakage; these results did not show as significant of an impact as expected. The physical model in the labs needs to be modified to incorporate a booster fan as part of the system. With this, a complete study using the booster fan can be conducted and the results compared to this study. Similarly, a CFD model should be calibrated to the upgraded system. The amount of work required to upgrade the existing CFD model developed for this study would be minimal. Continued research on the topic of leakage should include the use and optimization of booster fans.

APPENDIX A

ATKINSON'S FRICTION FACTORS FOR AIRWAYS AND RESISTANCE VALUES FOR VENTILATION CONTROL DEVICES

TABLE A.1 Suggested values for Atkinson's friction factor for coal mines (rectangular airways)

Source	k-factor, kg/m^3			Airway Description
Prosser and Wallace (1999)	0.0075			Clean with rock bolts, limited mesh
	0.0087			Some irregularities with rock bolts, limited mesh
McPherson (1993)	0.0090			Intakes, clean conditions, roof bolted
	0.0100			Returns, some irregularities, sloughing, roof bolted
	0.0050	-	0.0110	Belt entries
	0.0500	-	0.1400	Cribbed entries
	0.0350	-	0.0650	Longwall facelines
Bruce and Koening (1987)	0.0093			Intake
	0.0139			Return
	0.0278			Belt
	0.0186	-	0.6493	Longwall face
Hartman (from Kharker, 1974)	0.0046	-	0.0080	Smooth lined
	0.0080	-	0.0137	Unlined (rock bolted)
	0.0124	-	0.0167	Timbered

TABLE A.2 Suggested values for Atkinson's resistance values for individual ventilation control devices (Ns^2/m^8)

Source	Very Poor	Poor	Average	Good	Very Good	Description
Oswald, Prosser, Ruckman (2008)		1,786	3,329	5,311	6,628	Kennedy Stoppings
		2,425	4,691	7,758	10,674	Block Stoppings
Calizaya and Stephens (2006)		112	320			Omega block
		757				Kennedy Stoppings
			3,258	3,258		Concrete/Masonry
Schophaus, Bluhm, Funnel (2005)	100	300	1,000	5,000	25,000	
Bruce and Koening (1987)	1	112	559		781,900	Masonry Stoppings
			0.009			Single Overcast
					>1,117	Single Seal

APPENDIX B

METHOD OF CALCULATING POROUS MEDIA COEFFICIENTS FROM PRESSURE AND VELOCITY MEASUREMENTS

In Fluent, three factors define a porous jump zone: 1) face permeability, 2) porous medium thickness, and 3) a pressure-jump coefficient. Since experimental data of the pressure drop and velocity through the porous component are available, the porous media coefficients can be calculated (Fluent User's Guide, 2009):

$$\Delta \mathrm{P} = -(\frac{1}{\alpha}\mu \mathrm{V} + C_2 \frac{1}{2}\rho \mathrm{V}^2)\Delta n \qquad \text{(B.1)}$$

where:

P = pressure difference (Pa)

μ = fluid laminar viscosity (Pa·s)

ρ = fluid density (kg/m^3)

α = permeability of the medium (m^2)

C_2 = pressure jump coefficient (m^{-1})

V = velocity normal to the porous face (m/s)

Δn = thickness of the medium (m)

This process is described below using the data in Table B.1. The velocity and pressure data are used to generate a scatter plot and trend line through the points, yielding a 2nd-degree polynomial equation in the form:

$$\Delta P = AV^2 + BV \qquad (Pa) \qquad \text{(B.2)}$$

The resulting trend line coefficients A and B are 80.42 and 21.01, respectively. Substituting these values in Equation 4.3 yields the following relationships:

$$21.01 = (\frac{1}{\alpha}\mu)\Delta n \qquad \text{(B.3)}$$

Table B.1 Pressure and velocity measurements from three lab configurations using Gate #1

Fan Setting	Stopping Position	Velocity (m/s)	Pressure Drop (Pa)	Quantity (m^3/s)	Calculated Resistance (Ns^2/m^8)
60 Hz	A	3.26	1017.5	0.055	3.42E+05
	B	2.98	857.5	0.050	3.45E+05
	C	2.86	700.0	0.048	3.07E+05
	D	2.84	612.5	0.048	2.72E+05
45 Hz	A	2.49	575.0	0.042	3.31E+05
	B	2.39	467.5	0.040	2.92E+05
	C	2.13	392.5	0.036	3.11E+05
	D	1.55	337.5	0.026	5.01E+05
30 Hz	A	2.24	255.0	0.038	1.81E+05
	B	1.30	207.5	0.022	4.36E+05
	C	1.09	160.0	0.018	4.83E+05
	D	1.04	137.5	0.017	4.58E+05

$$80.42 = (C_2 \frac{1}{2}\rho)\Delta n \quad \text{(B.4)}$$

where

ρ = 1.01 (kg/m^3)

μ = 1.7894 x 10^{-5}(Pa-s)

Δn = 0.0031 (m)

The calculated pressure jump coefficient, C_2 is 50,157 m^{-1} and permeability, α is 2.70E-9 m^2. Although these coefficients are sometimes negative, in Fluent they should always be entered as positive values (ANSYS, 2009b).

Once the porous jump coefficients are known, the model can be calibrated. First the inlet pressure is set to the value measured in the lab. Then α and C_2 are adjusted by

trial and error until the measured values are replicated. Using this method there are many different solutions.

In FLUENT, the stopping gates may be modeled either as porous jumps, or, if the plate is thin, as porous jumps. In this case, the plates are 3.175 mm thick, so modeling each as a porous jump yields better convergence. The last open crosscut contains a wire-mesh screen that provides some resistance, so it too was modeled as a porous jump. For the last open crosscut, α is set to 2E+6 m^2 and C_2 is set to 134 m^{-1} (providing only slight resistance).

REFERENCES

1. ANSYS, Inc., 2009, *ANSYS FLUENT 12.0 Getting Started Guide.* ANSYS Workbench 12.0, ANSYS, Inc.

2. ANSYS, Inc., 2009, *ANSYS FLUENT 12.0 Theory Guide.* ANSYS Workbench 12.0, ANSYS, Inc.

3. Basu, A.J., Datta, D., and Gaur. P, 2004, "Design innovations for energy efficiency in underground mine ventilation," Presented at the 13th International Mine Planning and Equipment Selection Symposium, Wroclaw, Poland, September 1-3.

4. Bruce, W.E. and Koenning, T.H., 1987, "Computer modeling of underground coal mine ventilation circuits: selection and application of airway resistance values," *Proceedings of the 3rd US Mine Ventilation Symposium*, Penn State University, University Park, PA, pp. 519-525.

5. Calizaya, F., Karmawan, K., and K.G. Wallace, K.G., 2001, "PT Freeport DOZ mine ventilation system," *Proceedings of the 7th International Mine Ventilation Congress,* Cracow, Poland, pp. 949-953.

6. Calizaya, F., Duckworth, I.J., and Wallace, K.G., 2004, "Studies of air leakage in underground mines using computational fluid dynamics," *Proceedings of the 10th US/North American Mine Ventilation Symposium,* University of Alaska, Anchorage, pp. 417-424.

7. Calizaya, F. and Stephens, M., 2006, "Studies of leakage flow in the U.S. underground coal mines," *Proceedings of the 11th U.S./North American Mine Ventilation Symposium,* Penn State University, University Park, PA, pp. 599-606.

8. Calizaya, F., Stephens, M., and Gillies, S., 2010, "Utilization of booster fans in underground coal mines," SME Preprint No. 10-095. Littleton, CO: SME. Annual Meeting February 28-March 3, Phoenix, AZ.

9. Camber Corporation, n.d., www.cambergroup.com/mine.htm, Accessed February 2011.

10. Coetzer, W.J.J., 1985, "Use of a sealant paint to seal leakage through ventilation stoppings constructed from precast concrete bricks," *Journal of the Mine Ventilation Society of South Africa,* January 9-11.

11. Duckworth, I.J., Wallace G.K., and Wise R., 1995, "Ventilation planning and design of the Skyline mines," *Proceedings of the 7th US Mine Ventilation Symposium,* University of Kentucky, Lexington, pp. 9-14.

12. Federal Register, 2007, *Report of Investigation Fatal Underground Coal Mine Explosion, January 2, 2006, Sago Mine, Wolf Run Mining Company, Tallmansville, Upshur County, West Virginia, ID No. 46–08791*, Mine Safety and Health Administration.

13. Federal Register, 2010, Title 30 CFR Part 75 Mandatory Safety Standards – Underground Coal Mines. Subpart D – Ventilation, Code of Federal Regulations July 1 edition, http://www.msha.gov/30cfr/75.0.htm.

14. Francart, W.J., and Wu, K.K., 2002, "Ventilation," *SME Mining Reference Handbook,* Edited by Lowrie, R.L., Littleton, CO: SME, 259-274.

15. Gibbs Associates, 2002, www.miningsoftware.com, Accessed February 2011.

16. Hall, C.J., 1981, *Mine Ventilation Engineering,* Society of Mining Engineers of the American Institute of Mining, Metallurgical and Petroleum Engineers, Inc. New York, New York.

17. Hartman, H.L., Mutmansky, T.M, Ramani, R.V., and Wang, Y.J., 1997, *Mine Ventilation and Air Conditioning,* Third Edition, New York: John Wiley and Sons.

18. Kennedy, W., 1996, *Practical Mine Ventilation,* Chicago, Illinois : Intertec Publishing.

19. Kharkar, R., Stefanko, R., and Ramani, R.V, 1974, *Analysis of Leakage and Friction Factors in Coal Mine Ventilation Systems,* Special Research Report Number SR-99, Pennsylvania Department of Commerce.

20. Kawenski, E.M, and Mitchell, D.W., 1963, "An evaluation of stopping construction," *Mining Congress Journal,* September, pp. 57-61.

21. Kawenski, E.M., Mitchell, D.W., Berick, G.R., and Frances, A., 1965, *Stoppings for Ventilating Coal Mines,* US Bureau of Mines RI 6710.

22. Kawenski, E.M, and Mitchell, D.W., 1966, "Evaluation of materials for ventilation structures," *Mining Congress Journal,* March, pp. 49-53.

23. Mancha, R., 1942, *Effects of Underground Stopping Leakage upon Mine-fan Performance,* T.P. 1243 with discussion, New York Meeting.

24. Martinson, M.J., 1985, "Leakage between intake and return airways in bord and pillar workings," *Proceedings of the 2nd US Mine Ventilation Symposium,* Reno, NV, September 23-25, pp. 57-63.

25. McElroy, G.E., 1935, *Engineering Factors in the Ventilation of Metal Mines,* US Bureau of Mines Bulletin 385.

26. McPherson, M.J., 1993, *Subsurface Ventilation and Environmental Engineering*. London: Chapman & Hall.

27. Mine Ventilation Services, 2007, *VNETPC 2007 User's Manual and Tutorial,* Mine Ventilation Services, LLC.

28. Murphy, G., 1950, *Similitude in Engineering,* New York: Ronald Press, Co.

29. Oswald, N., Prosser, B., and Ruckman, R., 2008, "Measured values of coal mine stopping resistance," *Proceedings of the 12th U.S./North American Mine Ventilation Symposium*, University of Nevada, Reno, pp. 103-106.

30. Prosser, B.S., and Wallace, K.G., 1999, "Practical values of friction factors" *Proceedings of the 8th US Mine Ventilation Symposium,* University of Missouri-Rolla, pp 691-696.

31. Prosser, B.S., and Loomis, I.M., 2004, "Measurement of frictional pressure differentials during a ventilation survey" *Proceedings of the 10th US Mine Ventilation Symposium,* University of Alaska, Anchorage, pp. 59-66.

32. Ralph, A.M., and Nixon, T.R., 1983, "Ventilation survey procedures and database for use with computer simulation techniques," *Proceedings of the Australasian Institute of Mining and Metallurgy, Illawarra Branch Symposium,* Ventilation of Coal Mines, May.

33. Richardson, M.A., Gilbride, L. Adair, L., and Glasson, M.W., 1997, "Ventilation planning at the Aberdeen mine," *Proceedings 6th Int. Mine Ventilation Congress,* Pittsburgh, PA, pp. 33-38.

34. Sawyer, S. G. 1992, *Mortar for Use in the Construction of Concrete Block Stoppings and Seals in Underground Mines*, Mine Safety and Health Administration ISD Report No. 02-174-92, June 22, 13 pp.

35. Schophaus, N., Bluhm, S., and Funnall, R., 2005, "Effects of ventilation leakage in deep, hot room and pillar operations" *Proceedings of the 8th International Mine Ventilation Congress,* Brisbane, Austrailia, July 6-8, pp. 431-437.

36. Seeber, H.C., 2002, "Ventilation: understanding the factors affecting air resistance and their implications on mine operating and capital costs," SME Preprint No. 02-085, Littleton, CO: SME.

37. Singh, A.K., Ahamad, I., Sahay, N., and Varma, N.K., 1999, "Air leakage through underground ventilation stoppings and in-situ assessment of air leakage characteristics of remote filled cement concrete plug by tracer gas technique," *Journal of the Mine Ventilation Society of South Africa,* July/September, pp. 102-106.

38. Stefanco, R., 1983, *Coal Mining Technology, Theory and Practice.* Society of Mining Engineers, AIME.

39. Stephan, C. R., 1990, *Omega 384 Block as a Seal Construction Material*. Mine Safety and Health Administration ISD Report No. 10-318-90, 15 pp.

40. Strata Products Worldwide, LLC., 2010, www.strataworldwide.com, Accessed February 2011.

41. Tien, J.C., 1996, "Air leakage costs," *Coal Age,* September, pp. 88-96 and 121.

42. Timko, R.J., and Thimons, E.D., 1983, *New Techniques for Reducing Stopping Leakage.* US Bureau of Mines IC-8949, 15 pp.

43. Van der Bank, P.J., 1983, "Moving air from surface to the last through road in the section," *Journal of the Mine Ventilation Society of South Africa,* June, pp. 53-58.

44. Vinson, R.P., Thimons, E.D., and Kissell, F.N., 1977, *Brattice Window Method for Measuring Leakage Through Mine Stoppings,* U.S. Bureau of Mines RI 8240.

45. Wane, M.T., and Yegulalp T.M., 2008, "Coal mining," *AccessScience.* McGraw-Hill Companies, http://accessscience.com/content/Coal%20mining/143500, Accessed February 2011.

46. Weiss, E. S., Greninger, N.B., Stephan, C.R., and Lipscomb, J.R., 1993, *Strength Characteristics and Air-Leakage Determinations for Alternative Mine Seal Designs,* National Institute for Occupational Safety and Health Report of Investigation RI-9477.

47. Zipf, R.K. Jr., Sapko, M.J and Brune, J.F., 2007, *Explosion Pressure Design Criteria for New Seals in U.S. Coal Mines,* National Institute for Occupational Safety and Health Information Circular IC 9500, 76 pp.